NASA CR 166700

THE NASA STANDARD 20 AMP-HOUR NICKEL-CADMIUM BATTERY MANUAL

Contract NAS-5-23844
MMS Document No.
408-2101-0003

Prepared By
MCDONNELL DOUGLAS CORPORATION
ST. LOUIS, MISSOURI

TECHNICAL MONITOR
Gerald Halpert
Standard Battery Manager

Prepared For
The Modular Power Subsystem (MPS)
Multimission Modular Spacecraft (MMS)
GODDARD SPACE FLIGHT CENTER
GREENBELT, MARYLAND 20771

THE NASA STANDARD

20 AMP-HOUR NICKEL-CADMIUM BATTERY MANUAL

Project: MODULAR POWER SUBSYSTEMS

Submitted Under: NAS-5-23844

DATE 29 June 1979 PAGE ___ OF ___

REV A - 19 May 1980

		REV A
ORIGINATOR	D. A. Webb	
APPROVAL	J. E. Hallemann	
APPROVAL	W. D. Purdy	

CONTENTS

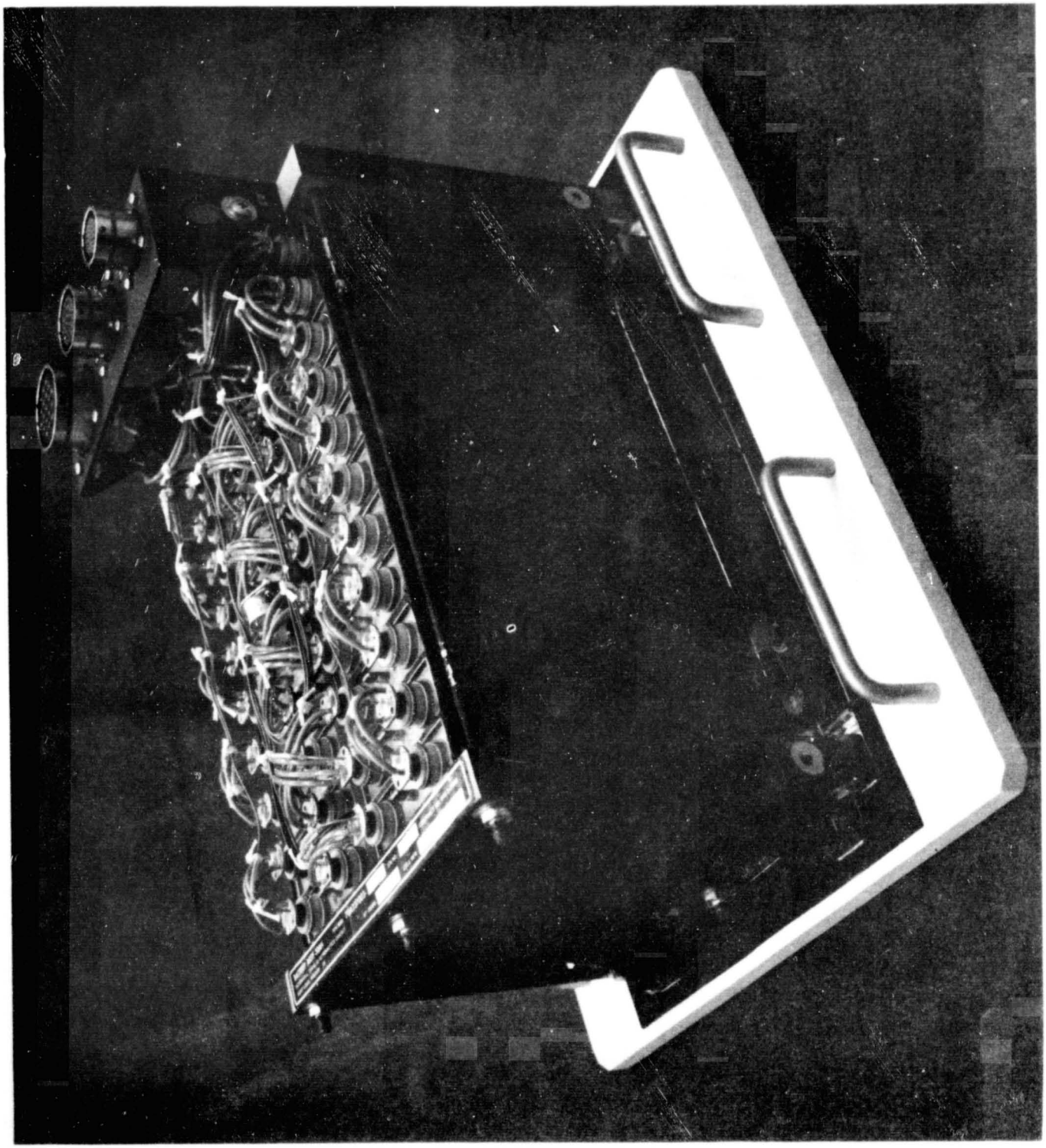

1 INTRODUCTION

The battery pictured on the preceeding page, is the 70A237003-1009 Nickel-Cadmium battery which was developed by McDonnell Douglas Astronautics Company-St. Louis for NASA Goddard as the NASA Standard 20 Ampere Hour Spacecraft Battery. The battery accommodates twenty-two cells. The cells are NASA Standard 20 A.H. Nickel-Cadmium hermetically sealed cells which are fabricated and tested in accordance with a comprehensive NASA Goddard approved cell manufacturing control document. The battery is designed with a minimum battery to cell weight ratio consistent with adequate containment for operating conditions and dynamic environments and minimized weight. The battery is fully qualified and the environments to which it has been successfully subjected were selected by NASA Goddard to cover a wide range of probable uses.

The battery is suitable for either near-earth or geosynchronous missions, is compatible with passive or active thermal control systems and may be electrically controlled by a variety of charging routines.

The initial application of the Standard Batteries is a near-earth mission aboard the Solar Maximum Mission Satellite.

2.0 CELL INFORMATION

2.1 General

The use of a NASA Standard Cell is a requirement of the NASA Standard Battery. At the present time only General Electric of Gainesville Florida is approved as a source of NASA Standard Cells.

General Electric manufactures the cells in accordance with Manufacturing Control Document 232A2222AA-84 Revision 8. The catalog number assigned the regular cell is 42B024AB06, while the signal electrode cell number is 42B024AB07.

2.2 Plaque

The plaque from which the plate is made contains a perforated nickel-plated mild steel substrate. A porous nickel is attached to the substrate by passing the substrate through a slurry containing powdered nickel-binder material mixture and subsequently through a sintering furnace. After sintering, the plaque is compressed and the plate coined areas are established.

Subsequent to the compression, the plaque is chemically impregnated with active nickel or cadmium materials.

2.3 Plaque Loading

Specified loading of the positive plaque is 11.64±.6 grams/decimeter^2. This relatively light loading is beneficial in that it lessens the degree of plate growth and physical degradation characteristic of chemically impregnated positive plates. The negative plaque loading specification is 14.92±.65 grams/decimeter^2.

2.4 Plates

There are eleven positive plates and twelve negative plates within a cell. The total positive plate area, including coined areas and excluding tab protrusions, is 10.44 decimeters^2 while the like area of negative plates is 11.39 decimeters^2.

The positive plates contain 5 percent cobalt hydroxide which reduces polarization, raises overcharge voltage level and thus improves plate charge acceptance. The negative plates receive a special Teflon treatment which aids oxygen recombination, retards cadmium migration through the separator and allows addition of more electrolyte.

2.5 Active Material Utilization and Positive to Negative Ratio

After detailed visual inspection and acceptance of the blanked plate, temporary flooded cells are assembled and tested to determine utilization of the active material impregnated into the plaque.

Experience to date indicates that 70-75 percent of the theoretical maximum capacity of the positive loaded material is realized during this testing. The utilization of the negative loaded material is 75-80 percent of the maximum theoretical.

The sealed cell capacity of the final room temperature acceptance test is approximately 96 percent of the positive plate capacity of the temporary (flooded) cell tests. The negative to positive recoverable capacity ratio based on the temporary cell test results is in a range of 1.65 to 1.75 for these cells.

2.6 Separator

The separator material is Pellon 2505 (non woven nylon). An envelope formed from this material covers each positive plate. The cell pack, positive and negative plates, is wrapped as a unit with poly-proplyene before case insertion.

2.7 Electrolyte

The electrolyte is thirty-one percent potassium hydroxide (KOH) aqueous solution. Eighty five milliliters of this solution are added to each cell at activation. The free volume within the cell is approximately 50cc.

2.8 Signal Electrode

The Standard battery is required to contain a signal electrode cell. The signal electrode is a cell within the case which senses oxygen pressure and, when externally loaded, outputs an analog voltage, between zero and one volt, which is proportional to the oxygen pressure it senses.

2.9 Cell Case and Header

The cell case is a welded design made from 304L stainless steel .019 inches thick. The header is a brazed assembly of: 304L stainless steel cover; nickel 200 terminals, sleeves, caps and studs; alumina insulators; and 304 stainless steel comb. The ceramic to collar and stud braze is nickel-titanium while the collar to header braze is nickel-gold. The assembled cell is hermetrically sealed and the terminals are insulated from the case. The terminals are pretinned by the cell manufacturer as a final step to facilitate soldering of intercell connectors.

2.10 Cell Capacity and Weight

The capacity requirement is 24±2 Ampere hours. Characteristically the cell capacity average during final room temperature acceptance testing based on SMM flight battery cells was 24.6 Ampere hours and the average cell weight is 1.96 pounds.

2.11 Acceptance and Burn-in

The cells undergo 24 cycles in the pre-acceptance and acceptance test prior to delivery. Included in these cycles are:

a) Six formation cycles prior to precharge	.....
b) Two pressure stablization cycles post precharge	
c) Overcharge cycle	Pre Acceptance Test
d) Ten Burn-in cycles	
e) Overcharge cycle	.....
f) One 74°F cycle	
g) One 95°F cycle	Acceptance Test
h) One 32°F cycle	
i) One 74°F cycle	.....

3.0 Mechanical Information

3.1 General

Figure 1 is an expanded drawing of the battery. In the figure the relationship of the mechanical components of the battery are shown. The battery "case" consists of two endplates, two channels, four tie rods, ten thermal fins, a connector bracket and the silicone potting. The assembly is lightweight, rugged and compact. The thermal fin assemblies serve a mechanical function in that the cell inertia loads are sheared into the fin upright members by the silicone bond and the loads are reacted at the fin gussets by the constraint of the holddown channels which are bolted to the mounting surface. The endplate design is a flat plate with integral ribs and frame. The flat side is next to the cells and transmits cell pressure load to the ribs and frame. The ribs and frame, in turn, transmit the load to the six tension members where the load is balanced by an equal load from the other endplate. A drawing of the battery envelope and mounting hole battery requirements is in the back of the manual.

3.2 Materials

A listing of the mechanical components and the materials from which they are made is as follows:

Endplates	7075-T7351 Aluminum Alloy
Channels	7075-T7351 Aluminum Alloy
Tie Rods	303 Stainless Steel
Thermal Fins	3003-0 Aluminum Alloy
Connector Bracket	2024-T351 Aluminum Alloy
Silicone	RTV 560
Cells	See Cell Information

3.3 Assembly

Each cell header, terminal and punch off tube, is protected by a machined phenolic block attached to the cell during the bonding process. All metal surfaces to be bonded are primed with GE SS4004 primer to assure good physical adhesion of the silicon potting. Three bonding tools are used in battery fabrication. One for individual cell bond, another for subassembly bonding and the third for all up battery bonding. Each cell is encased with 2.5 mil. thick glass cloth and silicone potting in the initial step of assembly. These bonded cells, in groups of four, are nexted bonded into subassemblies, which contain one or three thermal fins. Height and base flatness are controlled during bonding by application of downward force to the phenolic blocks mentioned earlier.

The final battery bonding joins four subassemblies, six cells and two endplates. The resulting total potting thickness between a cell and an adjacent thermal fin is approximately .018 inches.

The bonded and cured battery is compressed by a 1600 pound force (31 lbs/in^2) and the tension members are tightened uniformly until the indicated share of the force applied by the machine decreases to approximately 1400 pounds. At this point the machine applied force is relieved.

Battery base flatness is measured and corrected as necessary to meet the .010 TIR requirement.

The electrical assembly consists of adding the instrumentation probe, thermal switch, intercell connections, connector bracket and wire harness to the bonded battery.

3.4 Mounting

The battery is attached with ten fasteners. The recommended hold-down channel bolts are ST3M571 close tolerance flange head bolts with a 220 KSI rating. The recommended torque for these bolts is 40-45 inch pounds. The recommended endplate attachment screws are NAS 1531 Socket Head Cap Screws and the recommended torque is 15-20 inch pounds. Refer to the drawing in the back of the manual for the mounting hole pattern. The above recommendations are based on a maximum standoff of the battery to the mounting surface of no more than 0.1 inches, .063 inches of which are thermal fin base thickness.

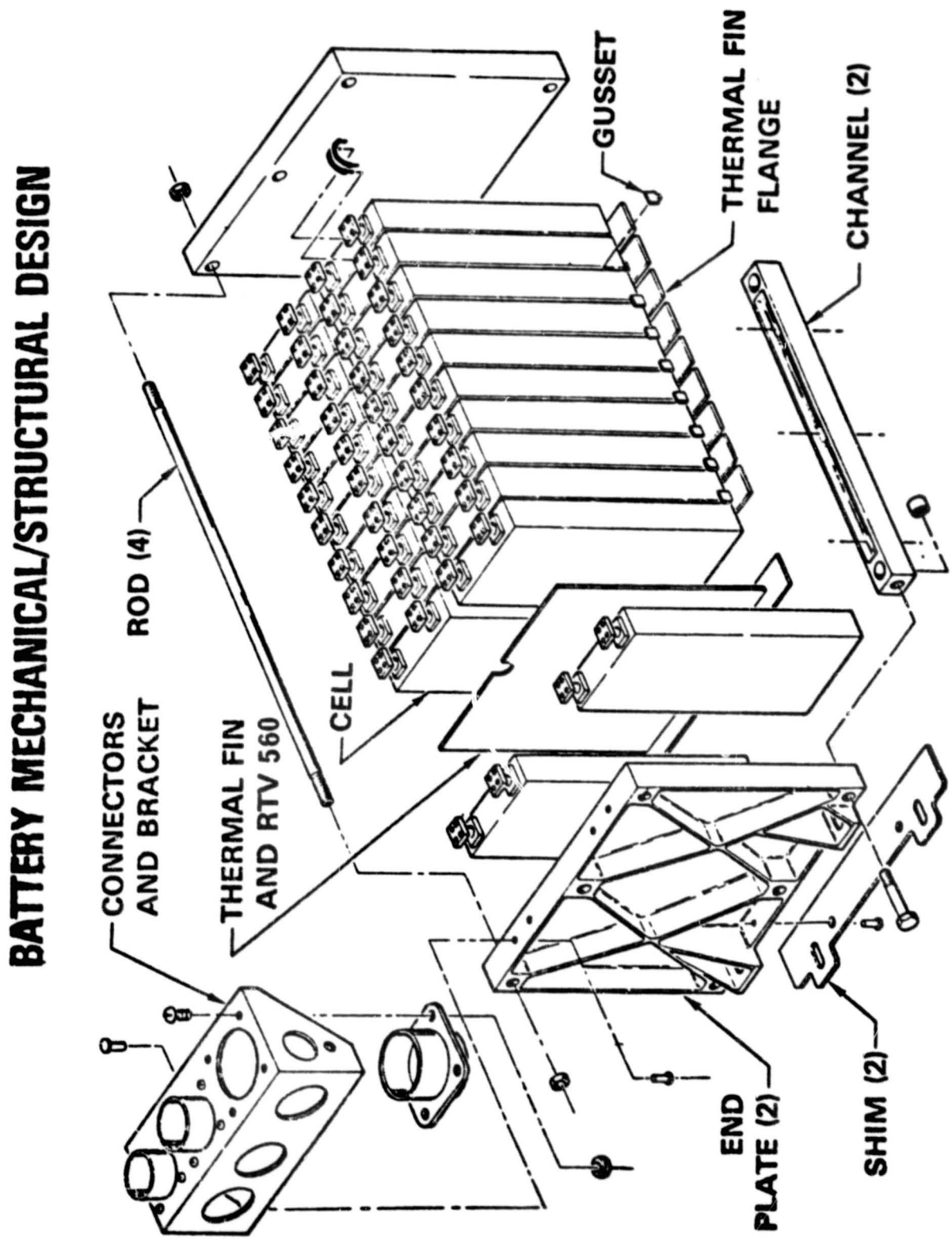
BATTERY MECHANICAL/STRUCTURAL DESIGN
GUSSET
THERMAL FIN FLANGE
CHANNEL (2)
ROD (4)
CELL
CONNECTORS AND BRACKET
THERMAL FIN AND RTV 560
END PLATE (2)
SHIM (2)

FIGURE 1

3.5 Battery Weight/Center of Gravity/Moments of Inertia

Completed battery weight is 52.6 pounds with the center of gravity very near the geometric center of the cell block. The Qual battery center of gravity and moment of inertia measurements are as shown in Figure 2. The products of inertia are insignificant.

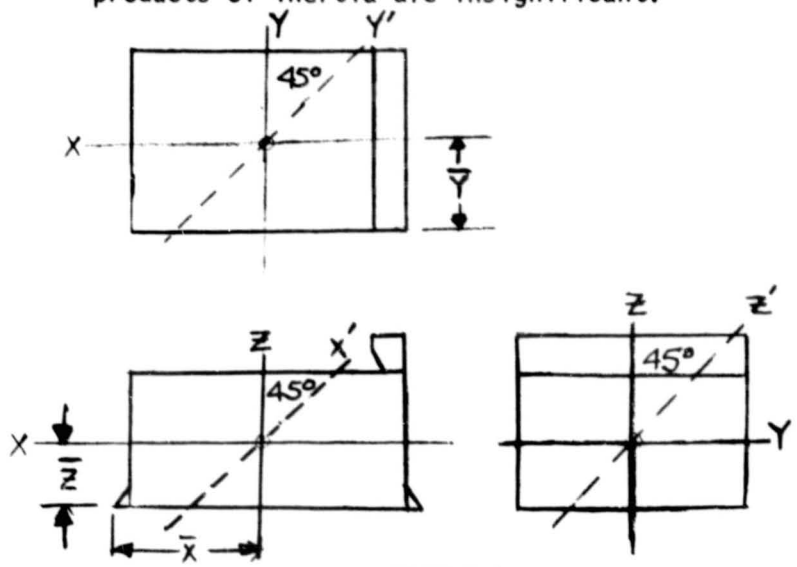

FIGURE 2

CENTER OF GRAVITY

$\bar{X}$ = 6.752 inches
$\bar{Y}$ = 3.899 inches
$\bar{Z}$ = 3.265 inches

MOMENTS OF INERTIA THRU C.G. ABOUT AXES INDICATED

MAJOR ORTHOGONAL:
I_X = .085 slug-Ft^2
I_Y = .162 slug-Ft^2
I_Z = .160 slug-Ft^2

45° CANTED:
$I_{X'}$ = .117 slug-Ft^2
$I_{Y'}$ = .122 slug-Ft^2
$I_{Z'}$ = .162 slug-Ft^2

3.6 Battery Dimensions

The overall dimensions indicated on the drawing in the back of the manual are maximums.

3.7 Maximum limit loads

The maximum limit loads used to design the battery structure occur independently and are:

a) Internal cell pressure of 100 psi
b) Acceleration load of 33 g's applied along any of the three orthogonal axes in either direction
c) Vibration levels as indicated in Section 4.6 of NASA Goddard Specification S-714-17
d) Shock levels as specified in Section 4.7 of NASA Goddard Specification S-711-17.

3.8 Vibration Resonance and Amplification

The development evaluation was conducted on a battery instrumented with triaxial response accelerometers located as shown in Figure 3. The battery was mounted on a flat-plate (1 inch aluminum) test fixture which was attached to the electromagnetic exciter system.

The peak transmissibility in the vertical test axis was 1.0 from 5 to 200 Hz. From the random data a fundamental frequency of approximately 360 Hz was indicated and the approximate amplification was 5. The peak transmissibility in the laterial axis was 1.7 and increasing at 200 Hz.

The laterial random data had peaks at 230 to 250 Hz and the approximate amplification was 3.5. In the longitudinal direction the peak transmissibility was 8.0 at 175 Hz.

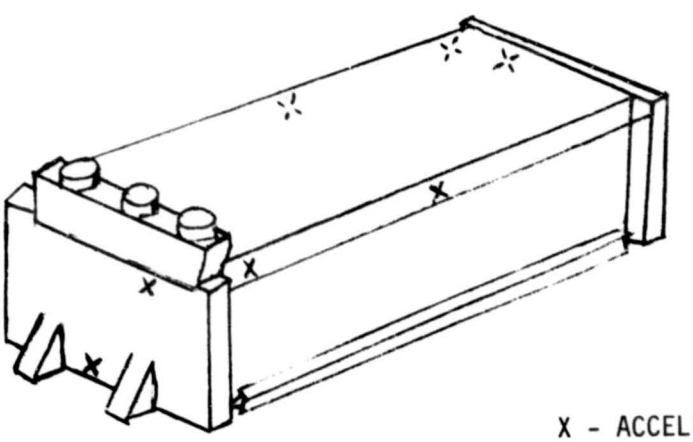

ACCELEROMETER LOCATIONS
DEVELOPMENT BATTERY EVALUATION

FIGURE 3

4.0 ELECTRICAL INFORMATION

4.1 General

Vendor acceptance performance records for the first time are used to select cells to be assembled into a battery. Standardizing cell fabrication has permitted the cost effective approach.

Silicone potting between the cell cases and the thermal fins or endplates accomplishes both mechanical and electrical objectives. Cell insulation from chassis and other cells is in the order of 10^6 megohms when tested at 100 VDC.

Twenty-two cells are electrically connected, after battery bonding, in a series string using MIL-W-81381 stranded 12 gauge wire jumpers Three jumpers, soldered between opposite polarity terminals on adjacent cells, provide strain relief, low resistance connection and ample current carrying capability.

Battery temperature sensor leads, signal electrode output, individual cell voltage sense leads and battery full and half voltage taps are routed to battery interface connectors to be used as condition indicators or battery control.

Unpainted areas are provided on the endplates for direct chassis grounding and battery chassis connections are routed through contacts on the power and signal connectors. The exposed areas, cell case tops, terminals and wire attachments are insulated (conformal coated) as the final manufacturing step in the battery assembly.

4.2 Cell Matching

Cells are selected for battery use based on their performance during cell vendor acceptance testing and their common plate lot origin. The voltage and capacity performance during the 32°F and the second 74°F capacity cycles are the data evaluated in the process. Normally the cells are tested in series connected groups of 25. Individual cell voltage and capacity variations from the group average are determined. These variations are then used to establish composite voltage and capacity distribution curves for the cells from the plate lot. A (A) battery's cells are then selected according to their grouping on the composite distribution curves.

Seventy five cells formed the base for matching cells for 3 SMM 22 cell flight batteries and the summarized results are as follows:

BTRY S/N	PERCENT FROM 22 CELL AVG. 74°F CAPACITY HIGH CELL	74°F CAPACITY LOW CELL	32°F CAPACITY HIGH CELL	32°F CAPACITY LOW CELL	END OF CHARGE MILLIVOLT DIFFERENCE FROM 22 CELL AVG. 74°F VOLTAGE HIGH CELL	74°F VOLTAGE LOW CELL	32°F VOLTAGE HIGH CELL	32°F VOLTAGE LOW CELL
A003	+0.9	-1.8	+2.6	-2.7	+5	-7	+2	-4.0
A004	+1.8	-1.8	+2.3	-2.3	+6	-7	+2.6	-3.4
A005	+1.9	-1.9	+2.1	-1.9	+5	-5	+3.5	-2.5

(A)

4.3 Electrical Interface

There are three scoop proof MIL-C-38999 type connectors on the battery and the connector part no. pin number, gauge, and functions are as stated below:

(J1) Power Connector - LJTPQOORT-25-19S453 (BENDIX)

Pin	Gauge	Function
V	12	Power Return
S	|	Power Return
P	|	Power Return
U	|	Power Positive
R	|	Power Positive
N	|	Power Positive
T	|	Btry Chassis
E	12	Btry Chassis

Remainder with unterminated contacts inserted with seal plugs in the grommet holes.

(J2) Signal Connector - LJTPQOORT-19-32S453 (BENDIX)

Pin	Gauge	Function
f	20	Cell 1 Positive
R	|	Cell 1 Positive
e	|	Cell 12 Negative
g	|	Cell 12 Negative
h	|	Cell 22 Negative
P	|	Cell 22 Negative
H	20	Btry + Sense

Pin	Gauge	Function
U	20	Btry + Sense
J	|	Btry - Sense
V	|	Btry - Sense
d	|	Signal Electrode Negative
c	|	Signal Electrode Positive
L	|	Platinum Resistor Terminal 1
K	|	Platnium Resistor Terminal 2
W	|	Platnium Resistor Terminal 1
X	|	Platnium Resistor Terminal 2
S	|	Thermistor 1 Terminal 1
T	|	Thermistor 1 Terminal 2
a	|	Thermistor 2 Terminal 1
b	|	Thermistor 2 Terminal 2
A	|	Thermistor 3 Terminal 1
B	|	Thermistor 3 Terminal 2
N	|	Thermal Switch Terminal 1
Y	|	Thermal Switch Terminal 2
M	|	Thermal Switch Terminal 1
Z	|	Thermal Switch Terminal 2
j	20	Btry Chassis Ground

Remainder with unterminated contacts inserted with seal plugs in grommet holes.

(J3) Test connector - LJTPQOORT-15-35S453 (BENDIX)

Pin	Gauge	Function
13	22	Btry (+)
15 Thru 25	|	Cell 1 (+) thru Cell 11 (+)
26 Thru 37	|	Cell 11 (-) thru Cell 22 (-)
14	22	Btry (-)

The 453 suffix in the connector part numbers assures the insert is a low outgassing material. The chassis of the battery has provisions for attachment of an external ground strap to the mounting surface.

4.4 Instrumentation

The instrumentation on the Standard Battery consists of a platinum resistor temperature sensor, three thermistor temperature sensors, a signal electrode in the most negative position cell, and a normally open thermal switch. The temperature sensors are potted into a .3 inch x 3.0 inch silicone cylindrical shaped probe which is subsequently bonded between the cells and abutting a thermal fin in the middle of the battery at cell top level. The platinum resistor is a Rosemount Engineering unit procured to a MDAC-STL source control drawing and has the following nominal characteristics:

Temperature	Resistance
-60°F	397.4 ± 2.00 OHMS
-8	455.6
+32	500.0
+44	513.3
+96	570.5
+148	627.1
+200	683.4
+212°F	694.9 ± 2.00 OHMS

The thermistors are Yellow Springs Instrument units and conform to NASA Goddard Specification S-311P-18. They have the following nominal characteristic:

Temperature	Resistance
-10°C	12.46K OHMS
0°C	7355 OHMS
+10°C	4482 OHMS
+20°C	2814 OHMS
+30°C	1815 OHMS
+40°C	1200 OHMS

The uniformity of the sensor indications is checked during battery acceptance testing at a stable temperature within ± 2°C of a target temperature. The tabulated results from an acceptance test show sensor uniformity.

BATTERY STABILIZED TARGET TEMP	PT. RESISTOR TS1		THERMISTORS TS2		TS3		TS4	
	Ω	TEMP	Ω	TEMP	Ω	TEMP	Ω	TEMP
0°C	501.6	.79°C	7097	.69°C	7093	.70°C	7136	.59°C
10°C	520.1	10.16°C	4482	10.0°C	4473	10.04°C	4483	10.0°C
20°C	539.9	20.14°C	2811	20.02°C	2806	20.06°C	2805	20.07°C

The thermal switch is a Sunstrand Data Control unit procured to a MDAC-EAST source control drawing. The switch has gold plated contacts suitable for low current circuit applications and closes at 35 ± 1.7°C. Reopening occurs at 30.6°C minimum. The minimum dialband between closure and reopening is 2.2°C. The oxygen sensing signal electrode terminals are loaded, on the battery side of the interface, with a 200 ohm resistor. Figure 3A and 3B are typical of the electrode signal during a 24°C capacity cycle.

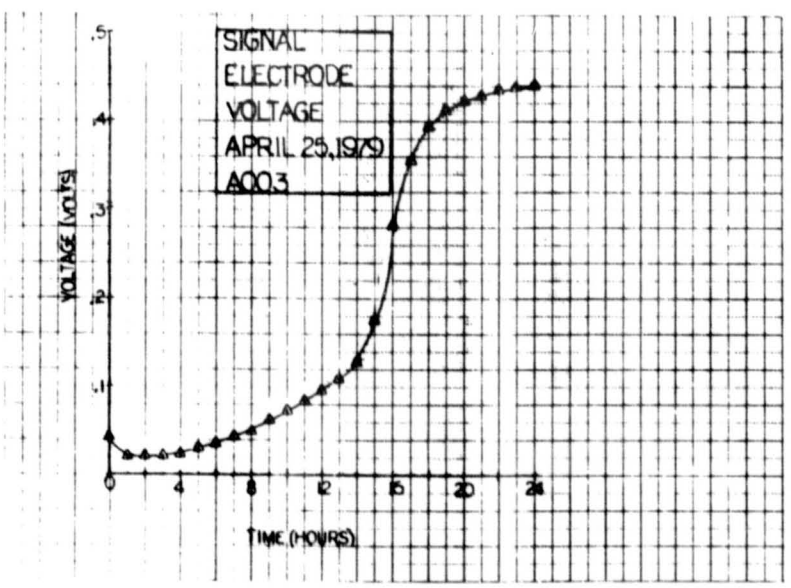

FIGURE 3a

ORIGINAL PAGE IS
OF POOR QUALITY

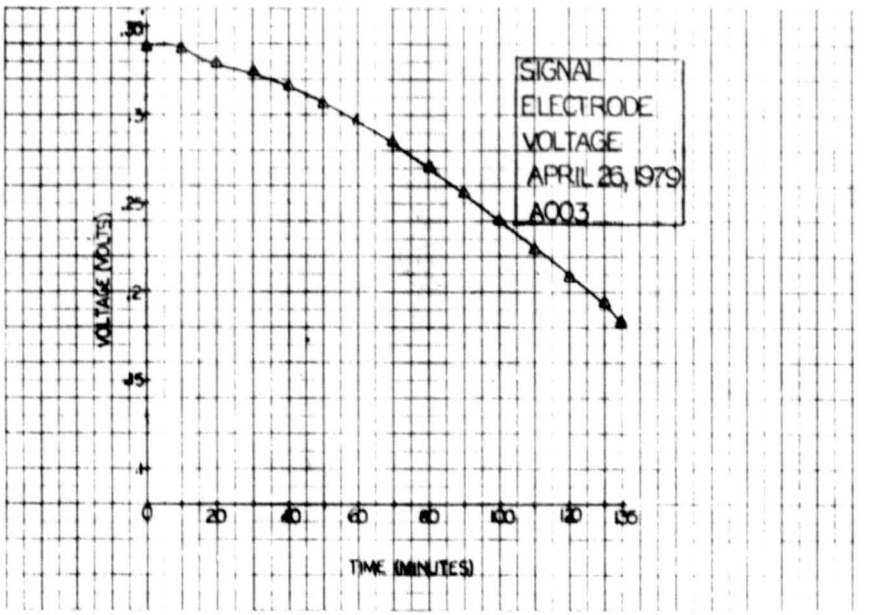

FIGURE 3b

4.5 Battery Capacity

A typical 24°C capacity profile for the Standard Battery is shown in Figures 4A and 4B. The capacities obtained from the first three flight batteries (SMM) are listed and are representative

BTRY S/N	CAPACITY	% VENDOR CELL AVG CAPACITY
A003	22.68 AH	92
A004	24.23 AH	98
A005	24.01 AH	98

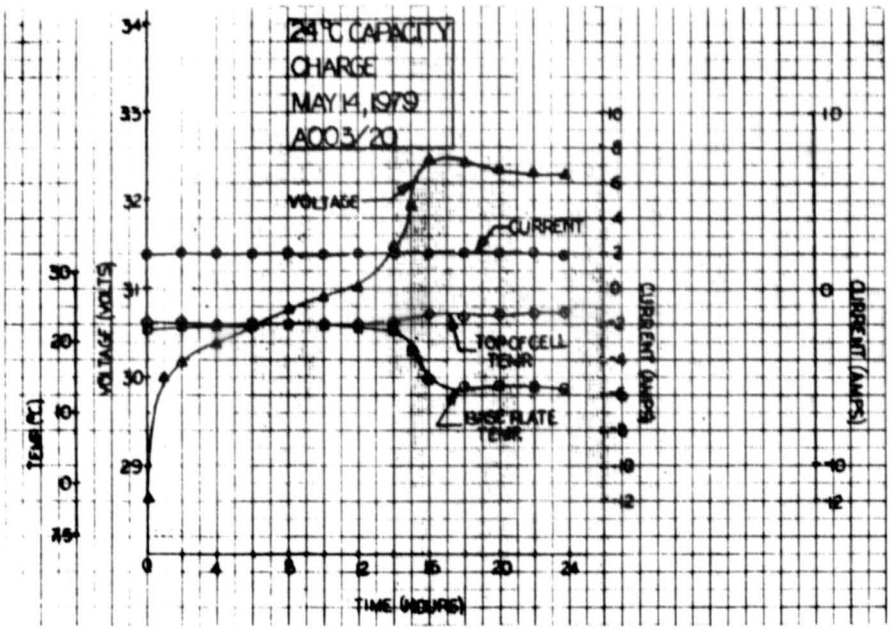

FIGURE 4a

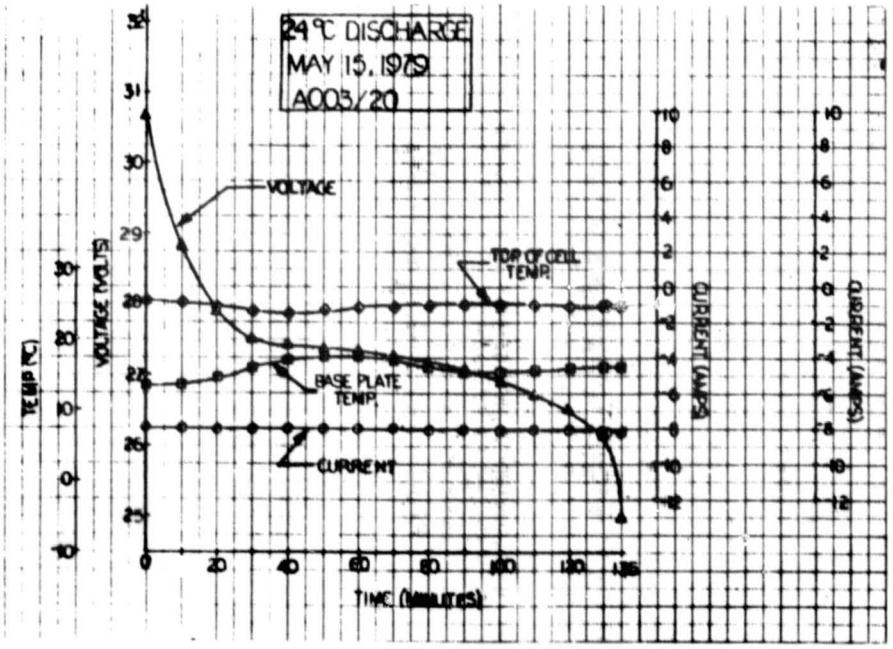

FIGURE 4b

A typical 10°C capacity profile is shown in Figure 5A and 5B. Representative capacities are:

BTRY S/N	CAPACITY	% OF INITIAL 24°C BTRY CAPACITY
A003	22.44 AH	99
A004	22.33	92.2
A005	21.96	91.5

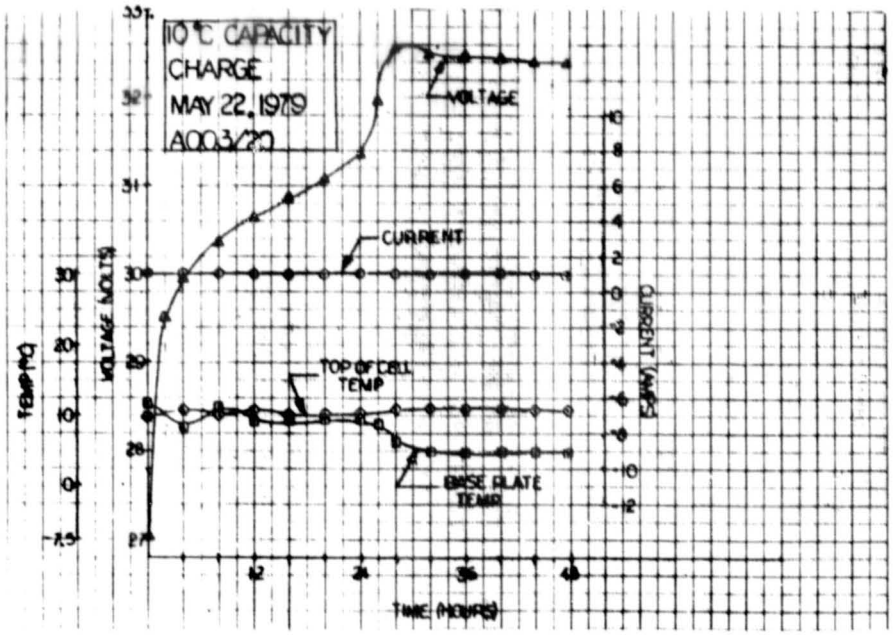

FIGURE 5a

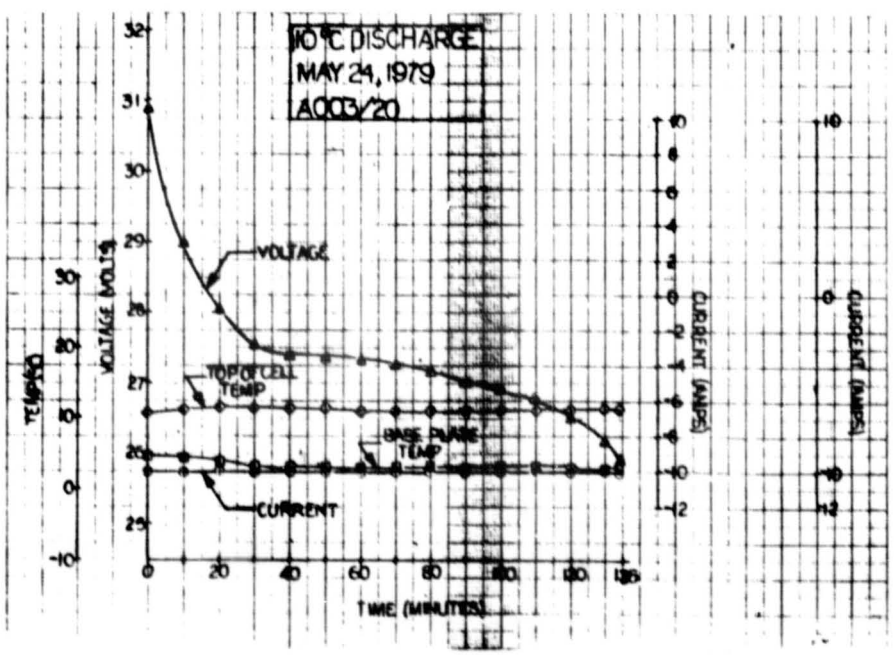

FIGURE 5b

A typical 0°C capacity profile is shown in Figures 6A and 6B. Representative capacities are:

BTRY S/N	CAPACITY	% OF INITIAL 24°C BTRY CAPACITY
A003	22.10 AH	97.4
A004	21.58	89
A005	21.12	88

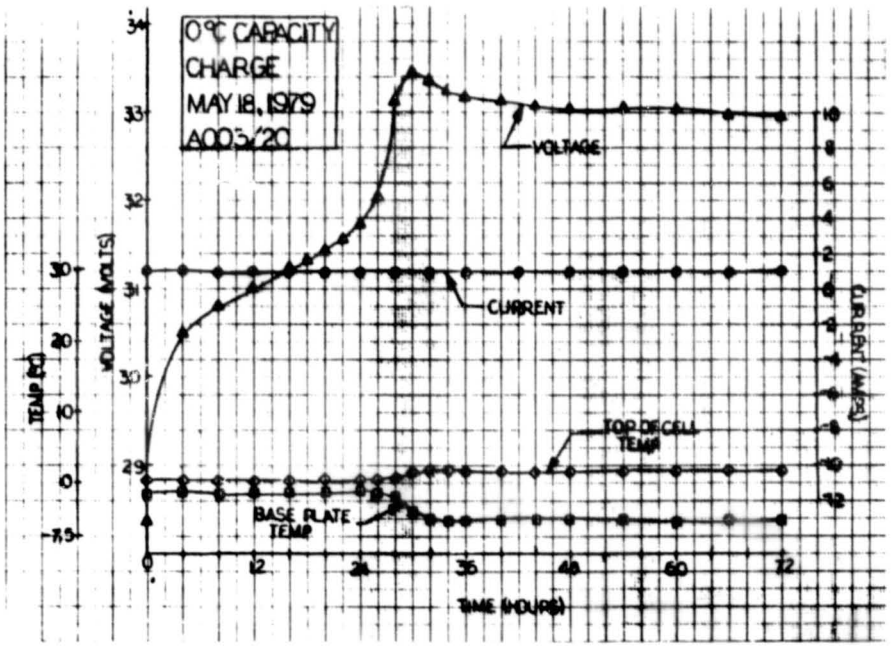

FIGURE 6a

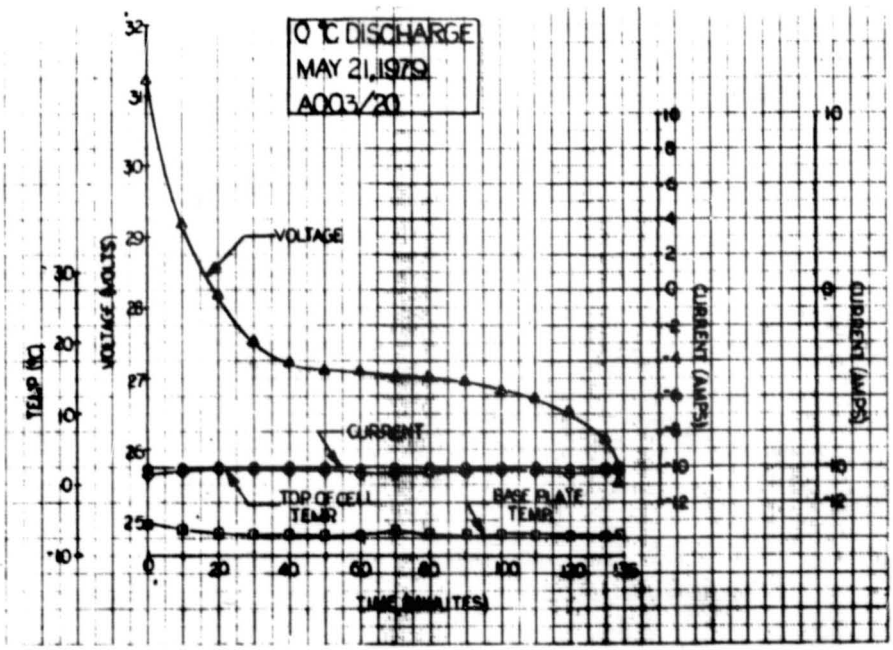

FIGURE 6b

4.6 Peak Load Performance

The Standard Battery performs well with high load current demands. During acceptance, the battery is subjected to a 5 minute load of 3C magnitude (60 Amperes) when it is at a 50 percent state of charge. The purpose of this test is to verify the integrity of all electrical connections within the cell and battery and disclose incipient separator weaknesses. The voltage and temperature response to the 3C load is shown in Figure 7. The calculated battery resistance ($\Delta V/\Delta I$) as a result of the 3C load application is 55 milliohms.

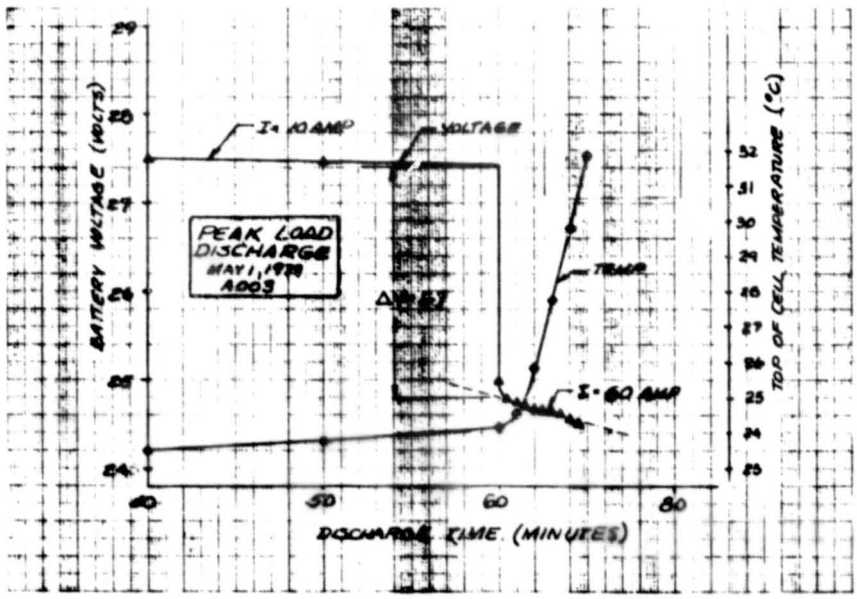

FIGURE 7

4.7 Orbiting Cycles and Charge to Discharge Ratios

Acceptance testing of the Standard Battery includes repeated 90 minute cycles at 25% DOD and 0°, 10° and 20°C mounting plate temperature. The batteries are in a 10^{-4} torr vacuum during these cycles. The cycling charge control routine begins with a constant C/2 charge current until the battery voltage reaches a pre-selected level (battery temperature dependent). From this point in the cycle until the next eclipse the voltage level is maintained and the charge current tapers. The discharge and recharge ampere hours are measured and cycling continues until the charge to discharge ratio reaches stability.

Typical data from these cycles are presented in Figures 8A, 8B and 8C.

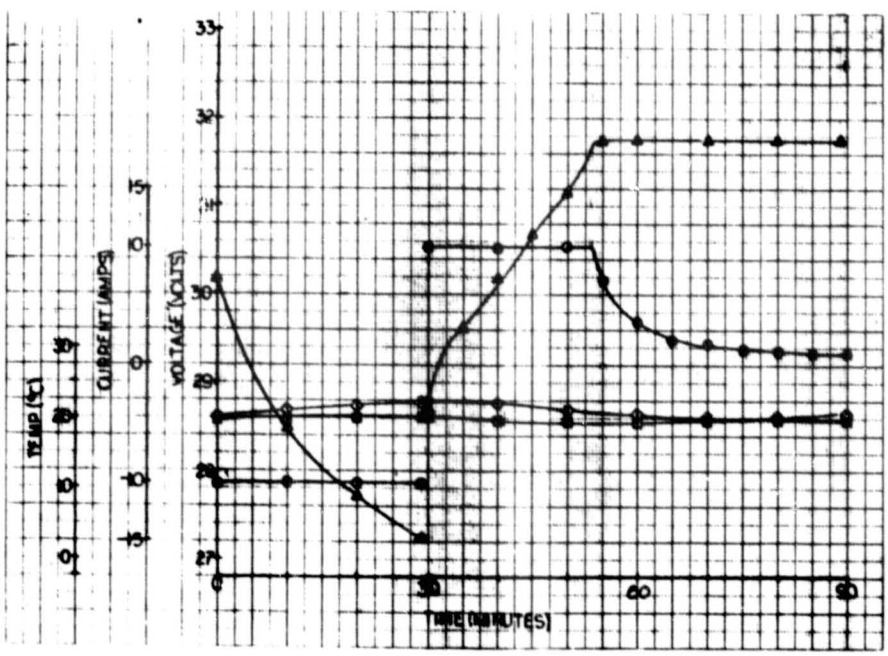

FIGURE 8a

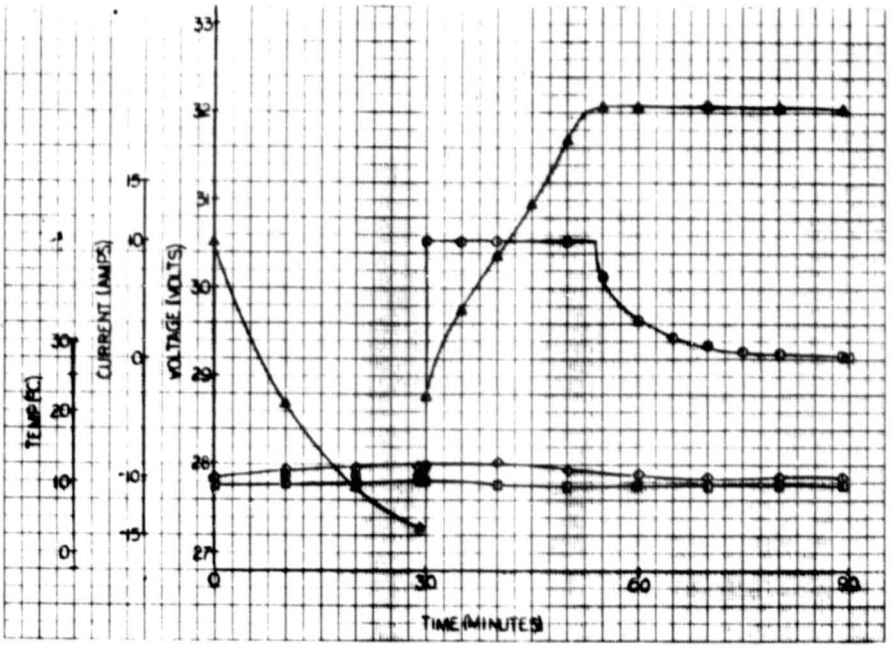

FIGURE 8b

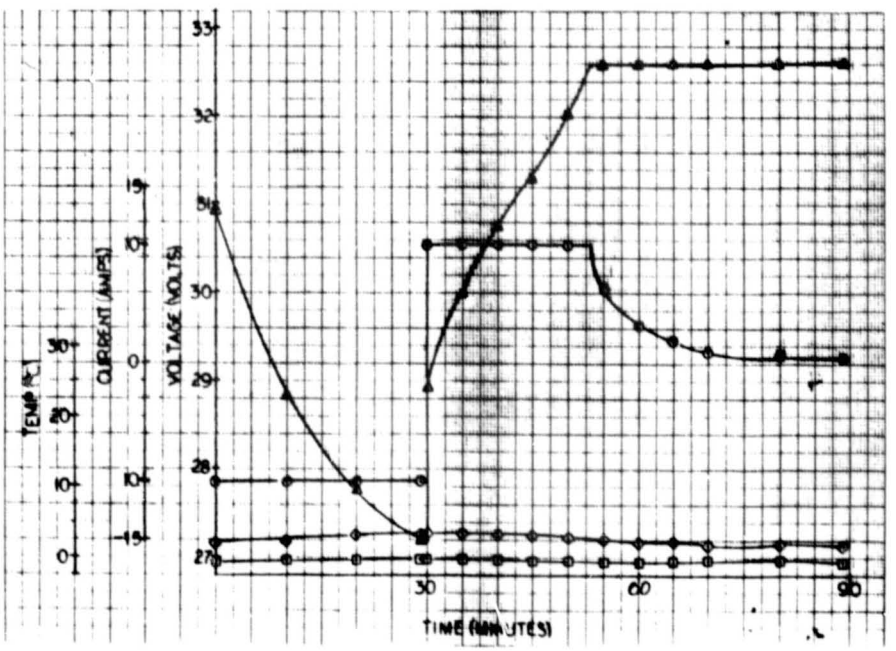

FIGURE 8c

The average charge to discharge ratios obtained during the acceptance cycling of SMM flight batteries are as follows:

Temp	Voltage Level	DOD	C/D Ratio
0°C	6	25%	1.023
10°C	6	25%	1.041
20°C	6	25%	1.078

The return ratio may be changed by selecting voltage limits other than level 6. This is the technique used to adjust the ratio to the range recommended by NASA Goddard to maintain the battery at a proper state of charge consistent with maximum available capacity, uniform cell performance and long battery life. See Figure 9.

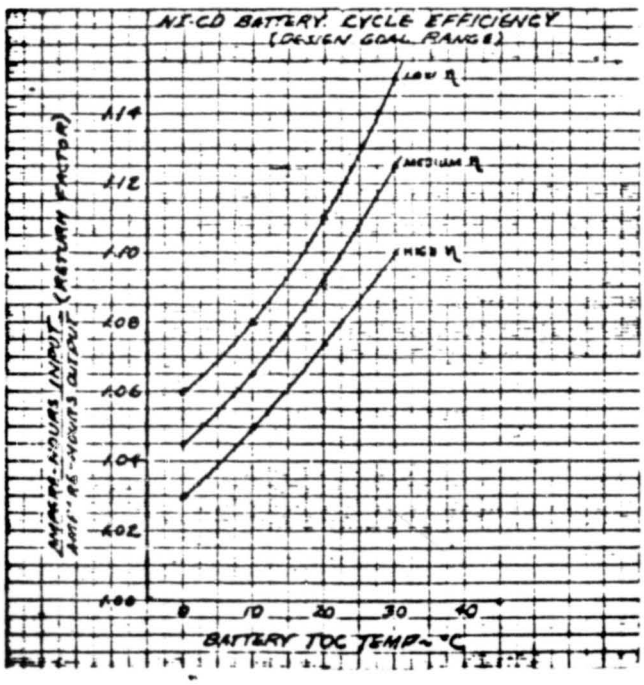

FIGURE 9

4.8 Battery Magnetic Properties

Batteries can contribute a considerable portion of a spacecrafts stray magnetic torquing moments if they contain large area wiring loops with appreciable current flow.

As can be seen in the introduction photograph, the Standard Battery contains five "crossovers" (crossed intercell connections) which create 2 pairs of opposing current loops and reduce the areas of the odd loop such that the resulting dipole moment with a C/2 rate current flow is within the S-711-16 Rev. A restraints.

5.0 Thermal Information

5.1 General

The 20 AH Standard Battery was designed to meet the thermal requirements of NASA Specifications S-711-16, Rev. A and S-711-17, which are the battery specification and qualification specification respectively. The thermal fin volume, bonding thermal characteristics, base flatness, cell arrangement and paint characteristics were selected to limit the thermal gradients within the battery to the 5°C top to bottom and 3°C difference in any plane parallel to the base.

5.2 Total Orbital Waste Heat Energy

To determine the total orbital waste heat energy generated by the battery, the user must consider his particular system application and make a judgement as to the battery cycle efficiency.

The battery depth of discharge and the users recharge technique are prime drivers in establishing a particular application's battery cycle efficiency.

Figure 9 represents the range of efficiencies covering most applications.

Once the application conditions have been established, the user may determine the total orbital waste heat energy as is done in the Addendum A paragraph 5 example.

5.3 Characterization

A thermal test was performed during the battery qualification process to characterize the battery's equilibrium heat transfer/heat storage properties over its normal operating range. Data were taken at constant levels of battery waste heat removal rate, but with controlled and widely different levels of internal heat generation rate. The evaluation of the results of this testing is presented in Figure 10.

Figure 10 includes the effective thermal mass of the battery as well as the effective thermal mass of the active coldplate used in the test. The effect of coldplate effective thermal mass inclusion is small and is considered representative of the contribution of other cooling system's thermal mass.

Derivation of Figure 10 relationships is covered in Addendum A "Evaluation of 20 A.H. Battery Thermal Performance During Qualification Testing.

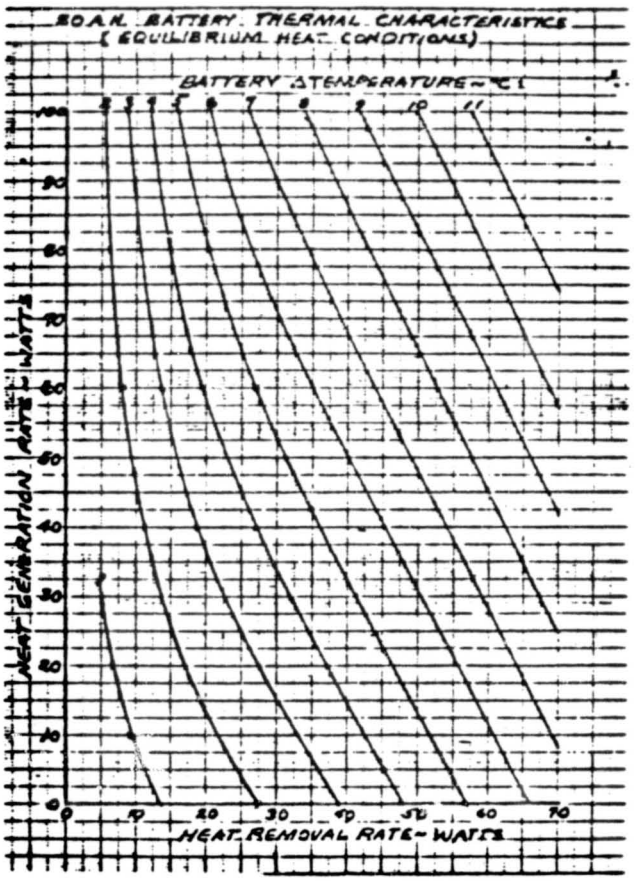

FIGURE 10

Knowledge of the average heat generation rate of the battery used in a specific application and of the average removal rate capability of the user's battery dedicated thermal system allows determination of the equilibrium gradient at averaged conditions directly from Figure 10.

Analysis of worst case orbital transient gradient conditions is possible using Figure 10 information and other application information i.e., depth of discharge, orbit times, transient radiator capability and battery recharge criteria preferences, which are unique to the user's system.

A typical use of Addendum A information in evaluating battery performance in an orbital operation application is found in Paragraph 5 of the Addendum.

6.0 Qualification

6.1 General

The qualification tests to which the 20 A.H. NI-CD Standard Spacecraft Battery has been subjected are listed in Table 1. The battery has successfully passed these tests and is fully qualified.

TABLE 1
QUALIFICATION TESTING

- Functional Tests
  - Temperature Sensor Operation
  - Thermostatic Switch Operation
  - Insulation Resistance
  - Conditioning
  - Leak Test
  - 24°C Capacity
  - Charge Retention
  - Peak Load
- Vibration/Shock
- Function Tests (As Above)
- Thermal Vacuum
  - Cycling
  - Thermal Characterization
- Capacity Tests
- Final Performance
  - Charge Retention
  - Peak Load
  - Temperature Sensor Operation
  - Thermostatic Switch Operation
  - Insulation Resistance
  - Leak Test
- Magnetic Properties
- Physical Measurements
- Humidity

6.2 Tests

Only those areas where ambiguity might exist or where levels are of interest are discussed below.

6.2.1 Capacity Tests

The battery top of cell temperature was maintained at the test temperature during charge and discharge. All discharges were conducted at the C/2 rate and were terminated when a 1.0 volt per cell average was reached or any cell reached 0.5 volts. Charging currents and durations were as follows:

Test Temp	Charge Rate	Duration
24°C	C/10	24 ± 1 Hr.
0°C	C/20	72 ± 1 Hr.
30°C	C/10	24 ± 1 Hr.
10°C	C/20	48 ± 1 Hr.

6.2.2 Charge Retention

This test was an open circuit, 24 hour voltage recovery type following 16 hour period of 1 ohm per cell shortout. Criteria was minimum of 1.17 volts per cell.

6.3 Vibration/Shock

Sinusoidal vibration was conducted along each major orthogonal axis at following levels:

Freq Range (HZ)	Level (Stated)	Sweep Rate (Oct/Min)
5-28	1.27 CM da	2
28-75	20 g	2
75-125	10 g	2
125-200	5 g	2

Random vibration was conducted along each major orthogonal axis for 2 minutes. Vibration was as follows:

Freq Range (HZ)	PSD (g^2/HZ)	Acceleration (g rms)
20-800	0.5	27.5
800-2000	-3 db/OCT	

Shock tests were along each major axis to the following spectrum level.

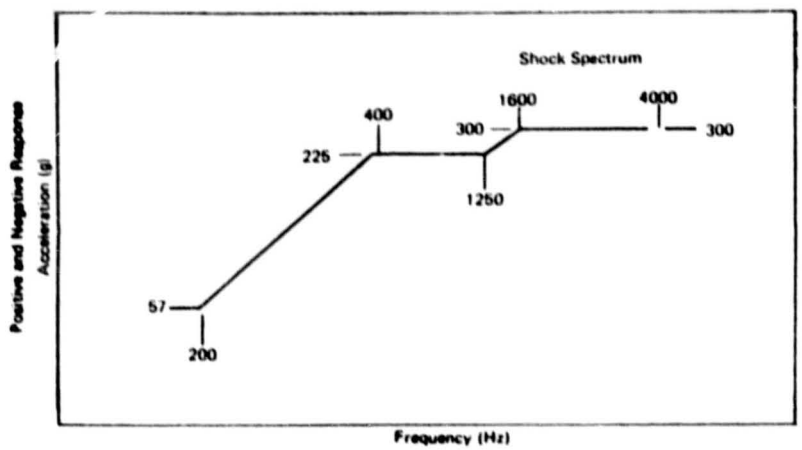

6.4 Thermal Vacuum

These tests were conducted at 10^{-5} torr with chamber walls at lab ambient temperatures.

6.4.1 Cycling

During cycling the battery top of cell temperature was controlled to the test temperature. Depth of discharge and voltage limit levels were as listed during the 30 minute discharge/60 minute charge cycles.

Test Temp	DOD %	CHG Volt Limit	BT Level
-10°C	10	1.463	4
-10°C	25	1.483	5
+10°C	25	1.457	6
+10°C	40	1.477	7
+30°C	25	1.411	6
+30°C	40	1.431	7

6.4.2 Characterization

The test method is outlined in Table 1 on page 3 of Appendix A.

6.5 Humidity

The battery, non operating, was subjected to a 30°C, 95 percent relative humidity environment for 24 hours. Prior to the test the battery, top of cells and terminals, were conformal coated and subsequent to the test a test was performed.

7.0 Acceptance

Acceptance tests are similar in scope to the qualification tests of paragraph 6. Differences are enumerated in following sub-paragraphs.

7.1 Vibration/Shock

The levels of exposure during sinusoidal and random vibration are decreased to two thirds of the qualification levels and the durations are decreased by 50 percent. Shock testing is not performed as an acceptance test.

7.2 Thermal Vacuum

Battery cycling in the acceptance test is performed at 0°, 10°, and 20°C and only at 25 percent depth of discharge. Voltage level 6 is used during acceptance cycling and battery base plate temperature is controlled to the test level.

7.3 Capacity Tests

Acceptance capacity tests are conducted at 0°, 10° and 24°C.

7.4 Magnetic Properties

This test is not performed in acceptance process.

7.5 Humidity

This test is not performed in acceptance process.

7.6 Physical Measurements

Determination of Center of Gravity and Moments of Inertia is not required in the acceptance process. Weight and dimensional measurement are performed.

8.0 Life Test

Near earth and synchronous life demonstration testing is being conducted by NASA Goddard in conjunction with Naval Weapon Support Center (Crane Ind.). There are four, four-cell packs and one, five-cell pack in this life test program. The four-cell packs are being tested for a near earth application at various temperatures and depths while the five cell pack is being evaluated for a synchronous application. A brief test condition summary is as follows:

Pack Ident No.*	Test Temp.	Repeated Cycle Depth	Orbit
12F	10°C	40%	90 Min
12G	20°C	25%	90
12H	20°C	40%	90
12I	30°C	40%	90
229A	20°C	60%	Synch.

* Number assigned to packs and used in the annual cycle life test report published by Naval Weapon Support Center, Crane, Indiana.

To date, approximately 11000 cycles have been accumulated on the near-earch specimens. In these tests, cyclic recharge is accomplished at C/2 constant current to a selectable voltage limit. The voltage limit mode is then maintained until the next scheduled eclipse. Every six months, the packs are capacity discharged, recharged and returned to cycling.

The synchronous evaluation pack is subjected to periods of cyclic operation twice yearly. The pack has been on test for approximately 2 years. During periods of continuous sun, the pack is charged at constant current of C/60.

9.0 Support and Handling Equipment

Support equipment (70D233006) is provided with each battery for protection of the battery heat transfer surface, cell terminals, instrumentation and battery wiring during periods of battery handling. A shorting connector (70D237018), which maintains each cell in hard shorted condition, is also provided. A battery, so protected, and shorted is packaged for shipment in a reuseable container (SC70A233005-501TD). The shipping container has temperature recording provisions internal to the outer box. The temperature recorder is a seven day recorder and provides a record of temperature profile throughout the period.

The inner box of the shipping container houses the battery, protective covers, and shorting plug which are wrapped as a unit with a sealed plastic covering (L-P-378). Within the inner box, and external to the plastic wrap, are (14) 4-unit bags of MIL-D-3464 Type II, non-dusting desiccant. The inner box is covered with a MIL-B-131 moisture barrier which is evacuated and heat sealed. The inner box, so sealed, is suitable for battery storage at 5°C ± 5°C.

10.0 Handling and Storage Recommendations

10.1 General

The following recommendations address storage and operational handling of all 20 AH-NICD Standard Batteries. The difficulty of rigid adherence to these recommendations for batteries installed in the using vehicle during checkout activities is recognized. For this reason, it is imperative that non-flight batteries serve as the power source during such activities and flight batteries be installed late in the launch preparations.

10.2 Storage

The recommended condition of battery storage, to assure minimal effect on its life and rate of performance degradation, is fully discharged with each cell individually shorted. Storage environment selection depends on whether the battery is installed or is being bench tested.

10.2.1 When to Store (Bench or Vehicle Installed)

Where it is determined a charged battery will be inactive for a period approaching a week, it is recommended the battery be discharged and the shorting plug installed until the scheduled usage at which time a regular C/10, 24°C, 24 hour recharge should be performed.

Where the anticipated inactive period exceeds a week and approaches 30 days, consideration should be given to placing the discharged and shorted batteries in a dry (<40% relative humidity), cool (5°C ± 5°C), storage area. Where the batteries are installed in a vehicle, an alternate to the above recommendations is to continually trickle charge the batteries during inactive period at a C/60 rate. Where the inactive period exceeds 30 days, the dry and cool storage should be used.

10.2.2 Removal From Storage

Batteries removed from cool storage should be allowed to stabilize at room temperature and precautions taken to preclude condensation accumulation. The recharge conditions are dictated by the length of battery inactivity. Special conditioning, C/20, 24°C, 48 hour charge and regular discharge, is required prior to the normal recharge if the period of inactivity exceeds 15 days.

10.3 Routine Installed Operation

Battery open circuit time should be minimized as it is deleterious to batteries. Where open circuit periods exceed four hours the battery should be discharged at a low rate (nominal spacecraft loads) for 2 to 5 minutes prior to attempting to charge. This will preclude slight hydrogen generation during initial moments of charge.

Operational time periods in excess of 14 days, where the battery(ies) have not been fully recharged and where their state of charge, due to random discharge and partial recharge cycles, is uncertain should be treated as follows:

a) Battery voltage under moderate load of <26.4 volts dictates a complete discharge (C/2 rate to 1.0 volt/cell avg. or any cell <.5 volts) and 1 ohm shortout of each cell for 16 hours followed by a C/10 recharge for 24 hours. CAUTION: Battery temperatures will rise during C/2 discharging and will also rise after approximately 14 hours of the C/10 charge. Cooling must be provided to maintain battery temperatures below 30°C. CAUTION: Battery discharging below terminal voltage of 25.75 volts with C/2 rate should only be attempted with individual cell monitor capability. Without this capability, the discharging should be terminated at 25.75 volts and each cell should be individually loaded with a 1 ohm resistor. Resistors should remain in place until battery terminal voltage is <3.3 volts.

b) Battery voltage under moderate load of >26.4 volts may be discharged for 2 to 5 minutes at the moderate load rate and then recharged at constant current charge (C/4) to voltage limit based on level 6 of S-711-16, Rev. A and then continued at that level until the current tapers to approximately C/10 level.

DEFINITIONS

Substrate	A .004 inch thick and seven inch wide mild steel strip which is approximately 85 percent perforated and subsequently nickel-plated.
Plaque	A substrate length which has porous nickel sinter attached and which is subsequently impregnated with active nickel or cadmium material.
Impregnation	Chemical process of inserting active material in the pores of the plaque nickel sinter.
Loading	The measure of active material chemically inserted in a given area of plaque. Generally given in grams per decimeter squared.
Plate	A processed portion of plaque containing an intergral non-sintered tab for attachment to cell terminal. Processing is a blanking operation where plate is cut to required shape.
Separator	Non woven nylon material used as electrolyte wick and electric insulator between positive and negative plates within a cell.

Addendum A

Evaluation of 20 AH Battery Thermal
Performance During Qualification Testing.

Addendum B

NASA Standard 20 AH Nickel-Cadmium
Spacecraft Battery

10/21/81

MODULAR POWER SUBSYSTEM

EVALUATION OF 20 A.H. BATTERY THERMAL PERFORMANCE DURING QUALIFICATION TESTING

21 OCTOBER 1981

CONTRACT NAS 5-23844

10/21/81

TABLE OF CONTENTS

1.0 SUMMARY

An evaluation of thermal performance data taken during the 20 A.H. battery qualification tests was made. Data taken at constant levels of battery waste heat removal rate, but with controlled and widely different levels of internal heat generation rate, was used to characterize the battery's equilibrium heat transfer/heat storage properties over its normal operating range.

This characterization was then applied to a design intended for operation in a low earth orbit. The effects on battery top-to-bottom temperature differential of the parameters: battery top-of-cell temperature, percent depth-of-discharge, battery charging return factor, and radiator heat removal capability, were examined over the range of potential interest for design. Those combinations of parameters which caused battery Δ temperatures over 5°C are shown. Maximum Δ temperatures occurred during the latter part of the discharge phase. At the beginning of the subsequent charge phase, Δ temperatures began to decrease rapidly.

The battery characteristics presented here can be applied to any type of orbital operation: i.e., they are not limited to the specific application demonstrated in this technical note.

2.0 INTRODUCTION

The 20 A.H. Standard Ni-Cd qualification test battery was instrumented and tested to the requirements of reference 2. These tests included three runs intended solely to provide battery thermal performance characteristics relating internal heat generation rate, heat removal rate, heat storage rate and heat storage capacity to the temperature differential from top to bottom at the battery.

The test battery was mounted on a circulating liquid coldplate. This assembly in turn, was installed in a vacuum chamber. The coldplate was instrumented as necessary to monitor and adjust the coldplate heat removal rate during the test runs. Temperature distribution within the battery was measured by instrumentation of fins at each end and at the center of the battery.

3.0 TEST APPROACH

The thermal vacuum test consisted of two types of testing, (1) battery cycle efficiency and electrical performance and (2) battery thermal performance. The latter type only is addressed in this technical note. The testing approach was to measure battery top-to-bottom temperature differentials as a primary function of heat removal rate for 3 classes of operating conditions representative of orbital operation:

1. Heat generation rate >> Heat removal rate
2. Heat generation rate = Heat removal rate
3. Heat generation rate << Heat removal rate

Heat removal rates covering the expected upper range of interest for orbital-average design were specified.

These tests were accomplished as three separate runs, each at a relatively constant level of heat removal rate as targeted in Table 1. Each run, in turn, was divided in three phases: (I) heat-up, (II) temperature stabilization, and (III) cool-down. A re-run of Phase I of Run 1 was performed at the end of Run 3 to confirm suspected low waste heat rate during the initial run. The three phases for each run were performed in a continuous sequence. Each run was preceeded by a "switch-over" period. During this period the battery was taken from a standby mode (for overnight or week-end storage) and "conditioned" for the test run. Temperature control was changed from the automatic constant-top-of-battery mode into a manual-reset mode. In addition, an overcharge power rate intended to match the cold-plate constant heat removal rate targeted for that run was supplied until battery top-to-bottom temperature differential approached its equilibrium value. At this time Phase I of the run could be started. The conditioning period thus (1) provided time to stabilize the cold-plate constant-Δ-temperature control mode and (2) also shortened the time required to reach battery Δ temperature equilibrium at the high, Phase I, over-charge power rates.

Values of the testing parameters used to control the test runs are provided in Table 1. The elapsed time estimates shown for each phase were intended to allow the battery and coldplate installation to reach an equilibrium mode during that phase. For the Phase II temperature balance, this was constant, but not equal, temperature levels throughout. For the Phase I heat-up, this was a constant (and uniform) rate of heat-up for the entire assembly. In like manner,

TABLE 1 - THERMAL PERFORMANCE TEST CONTROL PARAMETERS

GENERAL FOR ALL PHASES			
RUN NUMBER	1	2	3
CONSTANT HEAT REMOVAL RATE (qc) - WATTS	25	25	40
BATTERY CHARGER SETTING - VOLTS	$32.8^{+05}_{-0.0}$	$32.8^{+0.5}_{-0.0}$	$32.8^{+0.5}_{-0.0}$
PHASE 1 (HEAT-UP)			
INITIAL BATT TOC TEMP - °C	20±2	20±2	20±2
CONSTANT OVERCHARGE POWER/CURRENT RATE - WATTS/AMPS	50/1.60	75/2.39	80/2.55
TIME DURATION - HRS	1.5	0.75	0.92
PHASE 2 (TEMP BALANCE)			
INITIAL OVERCHARGE POWER/CURRENT RATE - WATTS/AMPS	25/0.81	25/0.81	40/1.28
FINAL OVERCHARGE CURRENT RATE - AMPS	AS REQ'D TO BALANCE TOC & ΔTEMPERATURE		
ESTIMATED ELAPSED TIME TO BALANCE - HRS	3	4	5
PHASE 3 (COOL DOWN)			
CONSTANT OVERCHARGE POWER/CURRENT RATE - WATTS/AMPS	12.5/0.40	8.3/0.27	20/0.65
TIME DURATION - HRS	2.5	2.5	2.5

the Phase III cool-downs were maintained until the entire assembly reached a constant and uniform cool-down rate.

In order to satisfy the test requirement for constant heat removal rate throughout any one run, manual adjustment of mixing value position to control coolant temperature into the coldplate was required often during the battery heat-up and cool-down phases. The most accurate assessment of heat removal rate is made by inputting measured values to the equation:

$$q_{cooling} = w\ C_p\ \Delta T \text{ in BTU/HR}$$

where w = coolant flow rate in #/hr

C_p = coolant heat storage coeff in BTU/#°F

ΔT = temp rise to coolant in °F

However, this is too cumbersome for real time control during battery heating and cooling. Therefore, since C_p and W vary by relatively small amounts during any one run, they were considered constant, and control was effected by holding to a constant level of coolant temperature rise in the coldplate.

Unlike the coldplate installation of reference 1, the installation used for these thermal runs was not configured as a calorimeter. Measurements of coolant flow rate and Δ temperature made during the test were intended primarily for real time control of heat removal rate to a relatively constant level and secondarily to hold this rate within the desired range of interest. A direct calibration of heat removal rate was obtained, however, during Phase II of each run by holding coldplate capacity constant and adjusting the overcharge power rate until a rate was found which maintained battery and coldplate temperature levels at constant levels for a nominal period of thirty minutes. This technique had proven to be more consistent than direct cold-plate calorimeter measurements for the tests of reference 1; and was therefore utilized for these tests. It was necessary, however, that the testing procedures insure essentially zero storage or unstorage of heat in the mass of the battery and coldplate; and no storage or unstorage of electrical power in the cells when the calibration data was taken.

The battery and coldplate were not insulated or shielded from the chamber walls. In order to minimize the corrections required for environmental (boundary) effects during Phase II heat balance testing, battery average temperature near

the end of the phase was kept near laboratory temperature ($\pm\Delta 7.0°F$ maximum). The heat rate balance for heat removal rate calibration was made at the interface of the battery base with the coldplate; where the heat removed at the base was set equal to the heat delivered to the base, i.e., heat generated within the cells plus or minus the heat gain or loss to the battery from its uncontrolled environment (at the sides, ends and top of the battery).

4.0 TEST RESULTS AND DISCUSSION

Tabulated data which was examined for this evaluation is presented in Appendix A. It includes time histories of pertinent instrumentation recorded prior to and during the 9 "equilibrium" operating periods targeted by the test plan outlined in Table 1. Also included in Appendix A are plots of the data as required to define battery temperature, heat storage, and heat transfer characteristics during these equilibrium periods.

The battery characteristics defined by this data were then used to normalize the separate and combined influence of battery heat generation rate and battery heat removal rate upon battery top-to-bottom temperature differential.

4.1 Data Description

That portion of the data which was examined in considerable detail for this evaluation is included as Appendix A. It includes tabulated time histories of temperature levels and differentials measured at the centerline of Fin #5 (center of battery). (These locations were determined during the reference 1 test program to produce higher top-of-cell (TOC) temperatures and larger top-to-bottom differential temperatures than any other location in the battery.) Coldplate inlet and outlet temperature levels are tabulated along with measured coolant flow rate. Time histories of overcharge current rate and battery voltage are also provided. All this tabulated data is presented in the chronological order in which it was taken. A re-run of Run #1, Phase I was performed immediately following Phase III of Run #3.

Plots of battery and coldplate system temperature data are also included as Pages A-1 through A-10 of Appendix A. These plots served two purposes not possible with the tabulated data. First, they were used to smooth and average out both the cyclical variations inherent in the refrigeration cart automatic control, and the step inputs to coolant inlet temperature which were being manually

TABLE 2

BATTERY POWER/HEAT IN.OT SUMMARY

TEST DATA POINT #	TEST RUN & PHASE #	BATT VOLT	BATT CURR	POWER INPUT	BATT AVG TEMP	BATT TEMP MINUS CHAMBER	RADIATION HEAT GAIN TO BATT	BATT TEMP RISE RATE	BATT HEAT STORE RATE	POWER IN LESS HEAT RADIATED	WASTE HEAT TO BATT BASE	BATT DIFF TEMP
		VOLTS	AMPS	WATTS	°F	°F	WATTS	°F/HR	WATTS	WATTS	WATTS	°F
1	1-I	31.95	1.60	51.1	68.7	+ 0.7	- 0.3	+ 3.4	+ 11.6	50.8	39.2	9.5
2	2-I	32.20	2.40	77.3	72.7	+ 4.7	- 2.4	+11.8	+ 40.1	74.9	34.8	12.4
3	3-I	32.26	2.55	82.3	73.0	+ 5.0	- 2.5	+ 6.85	+ 23.3	79.8	56.5	17.3
4	1R-I	32.25	1.60	51.6	63.7	- 4.3	+ 2.2	+ 4.55	+ 15.5	53.8	38.3	10.6
5	1-II	31.70	1.11	35.2	68.2	+ 0.2	- 0.1	0	0	35.1	35.1	7.5
6	2-IIB	31.65	1.19	37.7	72.8	+ 4.8	-2.4	0	0	35.3	35.3	8.3
7	3-II	32.14	1.75	56.2	70.5	+ 2.5	- 1.3	0	0	54.9	54.9	14.4
8	1-III	31.19	0.41	12.8	63.0	- 5.0	+ 2.5	- 5.2	- 17.7	15.3	33.0	5.6
9	2-III	31.04	0.27	8.6	63.0	- 5.0	+ 2.5	- 5.5	- 18.7	11.1	29.8	5.3
10	3-III	31.59	0.65	20.5	61.4	- 6.6	+ 3.3	- 7.3	- 24.8	23.8	48.6	10.0
11	2-IIA	31.56	1.11	35.0	73.0	+ 5.0	- 2.5	- 0.2	- 0.7	32.5	33.2	8.2

introduced throughout the test runs. Secondly, they were used to determine that an equilibrium battery/coldplate condition had been achieved for each phase, and had been maintained for a period of time long enough to confirm the temperature balance, a heat-up rate, or a cool-down rate according to what was targeted for that particular phase. The final results from these data plots are summarized in Table 2.

4.2 Heat Removal Rate Calibration

The primary objective of these tests was to determine battery top-to-bottom temperature differential as a function of both waste heat generation rate and waste heat removal rate. As discussed in Section 3.0 the testing approach was to measure battery Δ temperatures while cooling the battery at two different and constant levels (25 watts and 40 watts) and with heat being generated within the battery at different rates in the range from 8 to 80 watts.

Since the test set-up had not been configured to provide a heat flow rate calibration of the coldplate system, test procedures were developed which produced data permitting two other types of calibration of battery heat removal rate. Both depended upon determining the rate at which heat within the battery was being delivered to the base.

The first, and more direct, is obtained from the Phase II temperature balance data which zeroes out any heat storage in the battery and coldplate masses. At these conditions the heat rate resulting from overcharge, corrected for gains/losses at battery boundaries other than the base, is defined as equal to the rate of heat removal from the battery at its base. The data used for this calibration is plotted on pages A-2, A-5 and A-8, and the summary results are presented in Table 2 as Test Data Points #5, #6, and #7. These data points are also plotted as circled crosses on Figure 1 where they are used to define the battery characteristics curve for "calculated heat removal rate." This curve was drawn through Point #6 rather than #5, since the latter may have been taken before the battery reached its fully charged state and therefore may not have been converting 100% of the electrical power input into heat. Certainly this was true for the test phase immediately preceding it (Test Point #1), and that phase was repeated at the end of the thermal test series with the markedly different results shown by Test Point #4.

The second type of heat flow calibration, obtained from Phase I and Phase III data, depends upon establishing a constant and uniform rate of heat-up (or cool-down) of the total battery/cold-plate mass in order to derive a constant storage/unstorage heat rate which is applied as an additional correction to the boundary-corrected overcharge heat rate. The resultant heat rate is also defined as equal to the rate of heat removal from the battery at its base. The data used for this type of calibration is plotted on pages A-1, A-3, A-4, A-6, A-7, A-9, and A-10, and the summary results are presented in Table 2 as Test Data Points #1 through 4 and #8 through 11. These points are also plotted as crosses on Figure 1, where they tend to further confirm the heat removal rate calibration obtained from Test Data Points #5, 6 and 7. The results of Test Data Point #1 were questioned from the beginning, since the test installation did not heat up as fast as theoretically indicated for the excess heat which was being applied. Since this was the first phase of the first test run, there was reason to question whether the battery was fully charged. This phase was therefore repeated at the end of the thermal test series with the results shown by Data Test Point #4, which are considered much more satisfactory.

The crossed points of Figure 1 are plotted along lines extending from the corresponding circled point with a slope which represents the measured effect of a change in heat dissipation rate on battery Δ temperature while heat removal rate is held constant. In other words, the lines connecting the crossed points to the circled points are "lines of constant heat removal rate". Ideally, the crossed points would fall on the calibrated heat removal rate curve.

By what is considered theoretical necessity the calibrated heat removal rate curve of Figure 1 was extrapolated through point (0, 0). Extrapolation of this curve at the higher end above Data Point #7 very nearly touches the highest data point of the reference 1 test series (62 watts at 16.6°F Δ Temp).

There is some concern that this data did not generate a straight line for the "heat generated = heat removed" condition as in reference 1. Fortunately there is good agreement at the high waste heat levels where battery Δ temperature levels become most significant.

The calibrated heat removal rates of Figure 1 are generally higher than the rates targeted in the test plan. Further the rates vary somewhat from

a targeted constant value during each test run. Perhaps the most serious consequence of these deviations is that the test data results must be extrapolated farther on the lower end than originally planned.

4.3 Battery/Coldplate Heat Storage Calibration

In order to develop the second type of heat flow calibration discussed in Section 4.2, it was necessary to correct the heat flow rate data for heat storage effects measured during the heat-up and cool-down phases of the test. This heat storage correction was accomplished iteratively by selecting a value for battery and coldplate effective thermal storage capacity (in watt-hours per °C of equilibrium heat-up or cool-down) which provided the best fit to the measured data. This fit is illustrated in Figure 1 by the "crossed" points, where an ideal fit would have resulted if all eleven points had fallen on the "calibrated heat removal rate" curve. This storage calibration technique is considered quite reliable in that the test data points provided relatively large quantities of both storage and unstorage. The "calibrated" effective storage value thus obtained was 6.1 watt-hours per °C (3.4 watt-hours per °F) bulk temperature change. This value is 21% greater than the value calculated for the battery only in reference 1.

4.4 Battery Δ Temperature Characteristics

This section addresses the development of a characterization of maximum top-to-bottom temperature differential in terms of combined rates of heat generation within the battery and heat removal from the battery. The results for the measured data are extrapolated to some areas of potential interest.

For the second type of calibration of heat removal rate discussed in Section 4.2, it was necessary to determine the slopes of constant heat removal rate lines on a plot of heat generation rate versus battery Δ temperature (Figure 1). These slopes, passed through the appropriate points on the calibrated heat removal rate curve, were used to generate the parametric lines in Figure 2 for heat removal rates of 30, 40, 50, and 60 watts respectively.

Extrapolations of the basic test data results were made both to the waste heat generation rate and to the heat removal rate. The results are presented as Figure 3. In the extrapolation of heat removal rate downward to very low rates, it was assumed that the zero heat removal rate line must lie on the ordinate of the Figure 2 plot. This infers that heat is generated uniformly from the top to bottom of the battery and that if no heat were removed at the base, the battery would heat up uniformly. These assumptions may not be correct. On the other hand, the Δ temperature numbers thus obtained are quite probable, and are at a low level which is not likely to be critical to any real design installation.

The battery thermal characteristics of Figure 3 were crossplotted to show the same information in a different form on Figure 4. This form has parametric curves of constant battery differential temperature. This plot better illustrates the potential trades between heat generation rate and heat removal rate for a given level of battery Δ temperature; and the extreme Δ temperature penalty for removing high generation rates in real time. Figure 5 converts the battery Δ temperature scale of Figure 4 to ° Celsius.

5.0 APPLICATIONS TO ORBITAL OPERATION

The battery thermal characteristics descriptions developed from the test data in Section 4.0 are completely general and applicable to any type of battery usage for which the primary mode of heat removal is through the base and no heating of the battery from the base is intended as a design requirement. In this section, application of these thermal characteristics is made to a design intended for flight in a low earth orbit.

5.1 Operation In a Low Earth Orbit

5.1.1 Orbital and System Characteristics

The following characteristics form the basis of the application example to follow:

- o Orbit period equal to 90 minutes.
- o Occult period equal to 30 minutes.
- o Battery operating temperature (top of cell) average equal 20°C.
- o Battery effective thermal mass equal 6.1 watt-hour per degree C (see paragraph 4.3).
- o Battery depth of discharge (DOD) equal 25% of the rated capacity (C), where C equal 20 ampere-hours.
- o Battery charge routine is constant current (1.25C) until battery charge voltage reaches selected temperature compensated voltage limit. This voltage limit is maintained for the remainder of the charge period causing charge current to taper (decrease) to a low value.
- o Temperature compensated voltage limit in accordance with curve 6 of NASA Specification S-711-16.
- o Thermal system removes heat from the base of the battery at a constant rate equal to the orbital average waste heat generation rate.
- o Overcharge minimized such that all waste heat is generated in the discharge period.

5.1.2 Battery Recharge Efficiency

Battery orbital watt-hour effeciency must be established to continue the application example. Battery ampere-hour charge to discharge return factor envelope (amp-hour in divided by amp-hour out) for the battery at various temperatures is shown in Figure 6.

The ampere-hour ratio is a function of the temperature compensated charge voltage limit selected, orbit conditions, and the charge acceptance capability of the battery. In the application example it is assumed that the voltage level selected and the charge acceptance capability of the 20 A.H. battery results in operation corresponding to the high efficiency curve of Figure 6. Efficiently operating cells and carefully controlled recharging techniques are necessary to achieve the lower return factors represented by the lower (high η) curve.

The average charge to discharge voltage ratios, for the selected operating conditions of paragraph 5.1.1 were established from acceptance data of Solar Maximum Mission (SMM) Spacecraft batteries. (See figure 6A). The product of these voltage ratios and the ampere-hour ratios of Figure 6 results in the watt-hour ratio-temperature relationship depicted in Figure 6B for various battery efficiencies.

5.1.3 Discharge/Charge Average Heat-Generation Rates

Five ampere hours are removed from the application example battery during the occult period according to paragraph 5.1.1 conditions. (25% of rated (20 AH) capacity). The average 25% DOD discharge voltage for a 20°C battery during a 30 minute discharge period was determined from acceptance test data of the SMM flight batteries to be 28.35 volts. The electrical watt-hours removed in our application example is then 141.75 WH (5 AH x 28.35 V) and the total orbital waste heat energy generated is 24.66 WH (141.75 WH x (WH ratio 20°C -1)). In the application example all waste heat is relegated to the discharge period therefore the discharge period average heat generation rate is 49.32 watts (24.66 WH divided by .5 HRS) and the rate during charge is zero.

5.1.4 Thermal System Average Heat Removal Rate

The conditions in paragraph 5.1.1 state that the thermal system removes heat at a constant rate equal to the orbital average generation rate. In the application example this rate is 16.44 watts (24.66 WH divided by 1.5 HR orbit period).

5.1.5 Equilibrium Battery Temperature Gradients

The charge, discharge and orbital waste heat rates, thus determined, may now be applied to the general relationship developed in Section 4.0 (see figure 5) as has been done in Figure 7. Establishment of the dashed lines in the figure represent all limit operating points for the design application as long as the orbit length or percent of waste heat generated per phase are not changed. The

depth of discharge, average discharge voltage and battery watt-hour efficiency coupled with the requirement that the thermal system removal rate equal the orbital average heat generation rate establish a "typical operating line" as shown in the figure. Battery Δ temperature will always fall within the range defined by the end points of this line: The end point values will be experienced once during each orbit if the battery reaches the equilibrium heat-up and cool-down states. For this specific application study we have assumed that both minimum and maximum equilibrium will be realized. This is somewhat conservative with respect to maximum battery Δ temperatures. A test installation, which had a storage capacity of 6.1 watt-hours per °C, consistently reached equilibrium during a 1-hour cool-down period (sunlit charge phase). See Figure 8. However, it did not quite reach equilibrium in the half-hour heat-up period simulating the eclipse discharge phase. Time to full heat-up equilibrium was nominally 50 minutes for this test phase (see Figure 9). Even a battery with zero coldplate mass attached would have reached equilibrium only after 50/1.21 = 41. + minutes.

6.0 CONCLUSIONS AND RECOMMENDATIONS

6.1 A generalized characterization of battery top-to-bottom temperature differentials as a function of internal heat generation and base heat removal rates was derived from the test data. This differential is primarily determined by the heat removal rate, with a much smaller effect due to heat generation rate. The effect of internal heat generation rate is to increase the differential temperature if the generation rate exceeds the removal rate; and to decrease the differential if the generation rate is less than the removal rate.

6.2 The characteristics thus defined show battery differential temperatures to be as much a function of the vehicle or test installation as of the battery itself. Further, it is not difficult to postulate battery installations which would cause the battery to operate at differentials in excess of 5°C. The least optimum of these would remove heat even faster than it was being generated during the discharge phase; then add base heat during the sunlit (charge) phase, in order to get the battery bulk temperature back up to its repeating orbital value. The better installatiions would store part of the heat in the battery during periods of high waste heat generation, to be released when heat generation is low (or even negative). Fortunately, this latter type is more typical of space radiator installations, and the former type usually occurs only in ground test installations.

6.3 The characterization of Section 6.1 allows an integration of the battery characteristics with any potential vehicle or test installation to the extent that the heat generation and removal rates can be expressed as quasi-steady state values. The battery characteristics as presented are for combinations of heat removal and heat generation rates which were maintained until the battery reached a constant (equilibrium) level of top-to-bottom temperature differential. These values, then, are the maximum or minimum which would ever be reached regardless of the elapsed time. Battery operating conditions which are too transient to produce equilibrium battery Δ temperatures would therefore reach only intermediate levels; and would produce conservative limiting design criteria when evaluated directly against the generalized characterization.

For some of these transient conditions, it may be cost effective to develop a computerized transient thermal model of the battery, mounting provisions, and space radiator in order to prevent excessive conservatism in the vehicle installation design requirements.

6.4 The combined heat storage capacity of the battery and coldplate masses was measured as 6.1 watt-hours per °C bulk temperature change. This is 21% greater than the value calculated for the battery only.

6.5 The time to reach a new equilibrium top-to-bottom temperature differential within the battery following a step change in the combination of heat generation and heat removal rates, was approximately 50 minutes, whether the battery was heating up or cooling off. Since the equilibrium value was approached asymptotically, near-equilibrium was reached in about 40 minutes.

A proportionate reduction in time to reach equilibrium would result if the thermal mass of the vehicle installation were less than the battery/coldplate mass of the test installation.

6.6 Specific application of the data to a vehicle in low earth orbit was made to demonstrate the relative sensitivity of battery top-to-bottom temperature differential to variations in the design parameters of battery top-of-cell temperature, percent depth-of-discharge, battery charging return factor (battery cycle efficiency),and radiator heat removal capability. Limiting values were defined for possible combinations of these design parameters.

Application of test data results to missions other than low earth is, of course, possible. The low earth orbit is generally considered more critical to vehicle installation design, however, than the orbits at higher altitudes.

6.7 Considering the results of this evaluation, it is recommended that:

For any future tests intended to confirm adequate battery heat transfer/storage capabilities, the heat removal rate be controlled either to a constant level or to programmed levels simulating the design radiator characteristics most adverse to battery operation.

During the tests above, either simulated or actual variations of the design parameters of battery charging return factor (battery cycle efficiency), top-of-cell temperature, and percent depth of discharge be input, but only over the ranges and in the combinations essential to an overall weight- and cost-effective vehicle design. It is preferred that as many of these inputs as possible be by direct battery cycling; supplemental tests to define battery cycle efficiency versus battery charge control techniques, battery top-to-bottom temperature differentials, and battery bulk temperature levels are strongly recommended in any areas where these characteristics are not already well documented.

The sensitivity of battery electrical efficiency and storage capacity performance to battery top-to-bottom temperature differential be evaluated by test for both the charge and the discharge phases individually. (Battery temperature differentials peak at the end of the discharge phase, then decrease rapidly as charging commences. The battery may be much less sensitive to differentials at the end of the discharge phase than near the end of the charge phase, permitting a higher limit Δ temperature for this portion of the cycle and an easier installation design.)

REFERENCES

1. Technical Note No. 16, "Thermal Performance Evaluation of 20 A.H. Battery Development Tests," dated 5 November 1977.

2. TR 70A-101- "20 A.H. Standard NI-CD Battery Qualification Test Procedure," as amended by PCN #63, "Revision To The Thermal Vacuum Electrical Cycle Test," dated 17 February 1978.

FIGURE 1

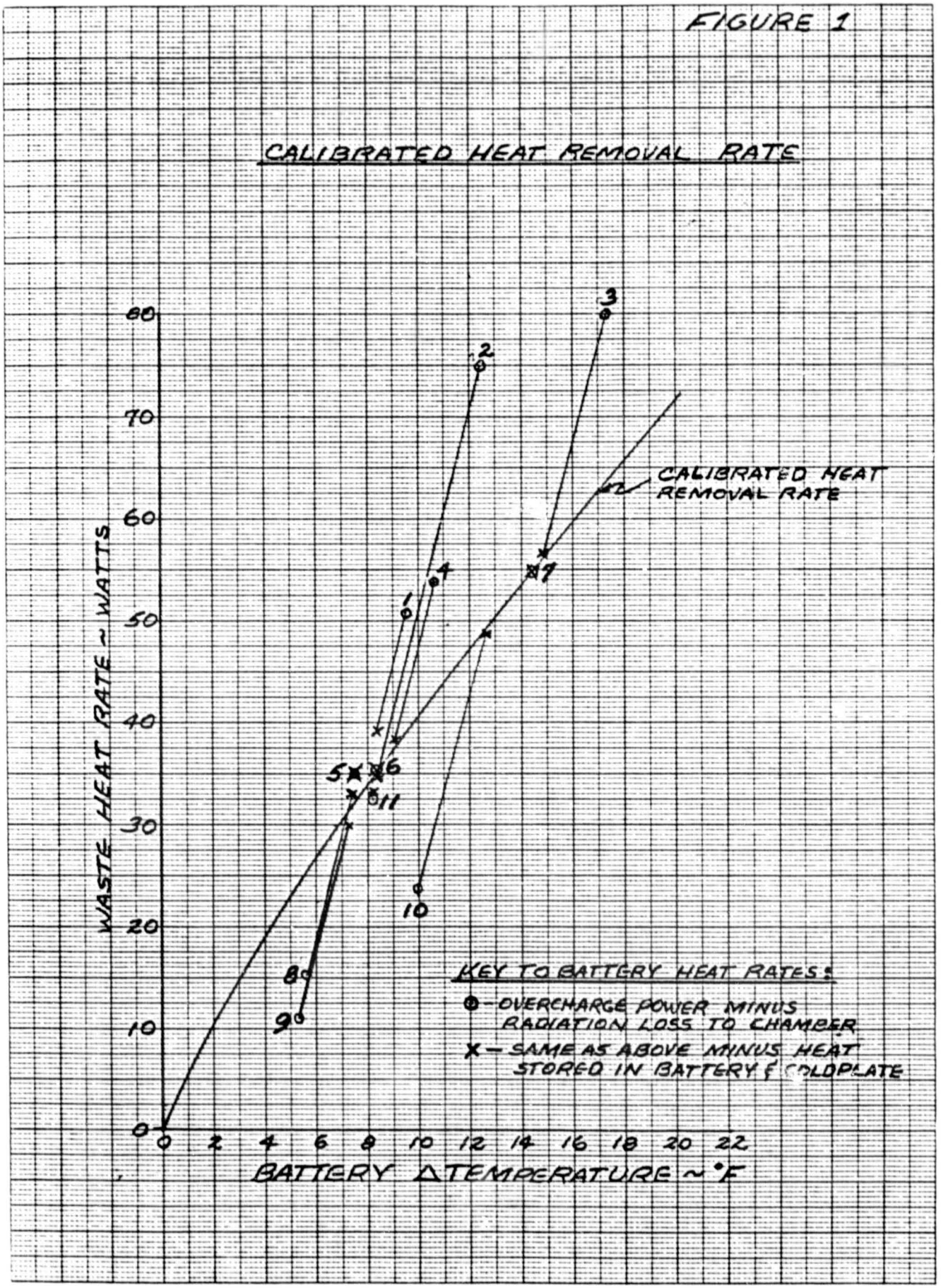

FIGURE 2

DERIVATION OF CONSTANT HEAT REMOVAL RATES FROM MEASURED DATA

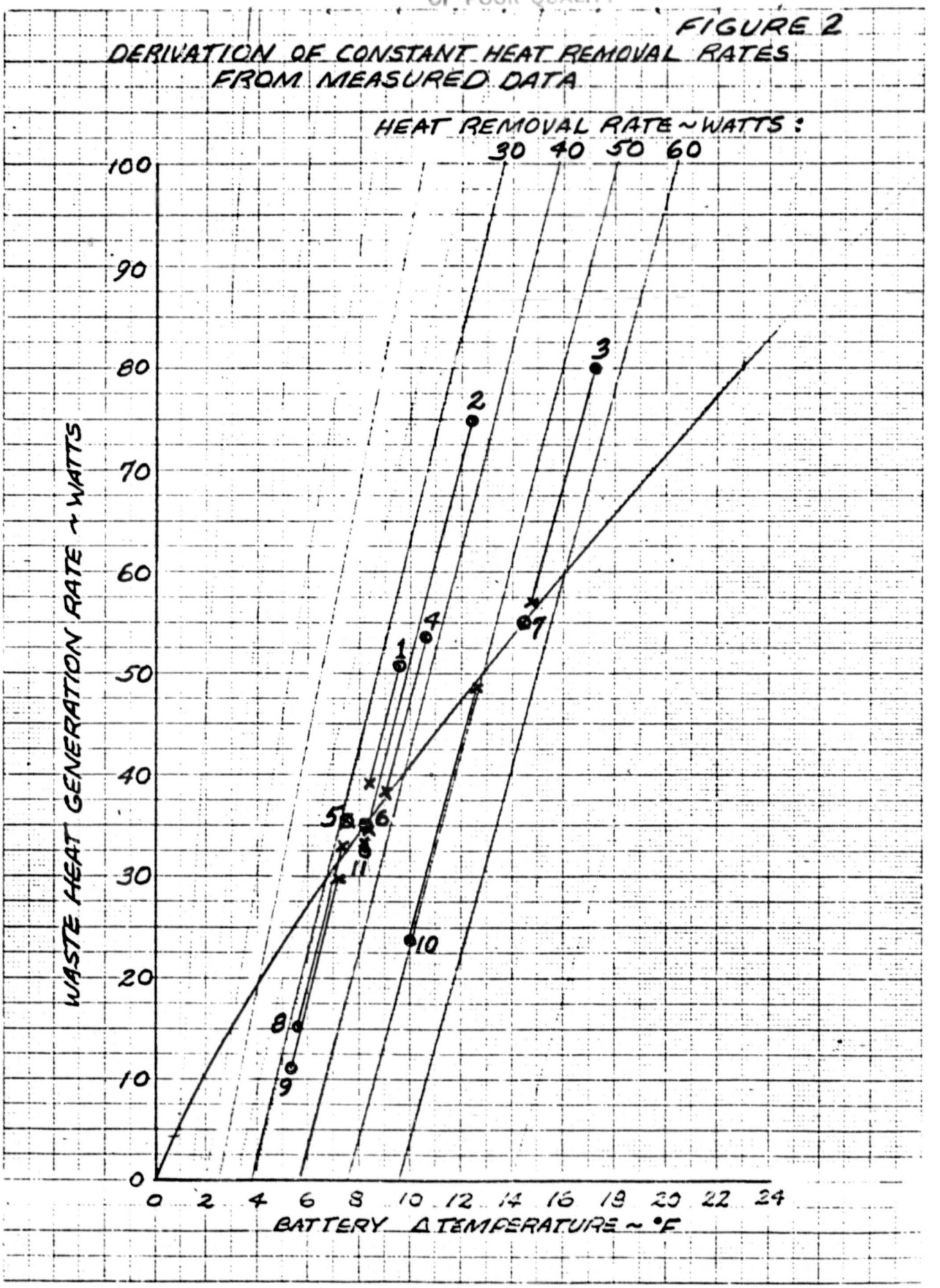

FIGURE 3

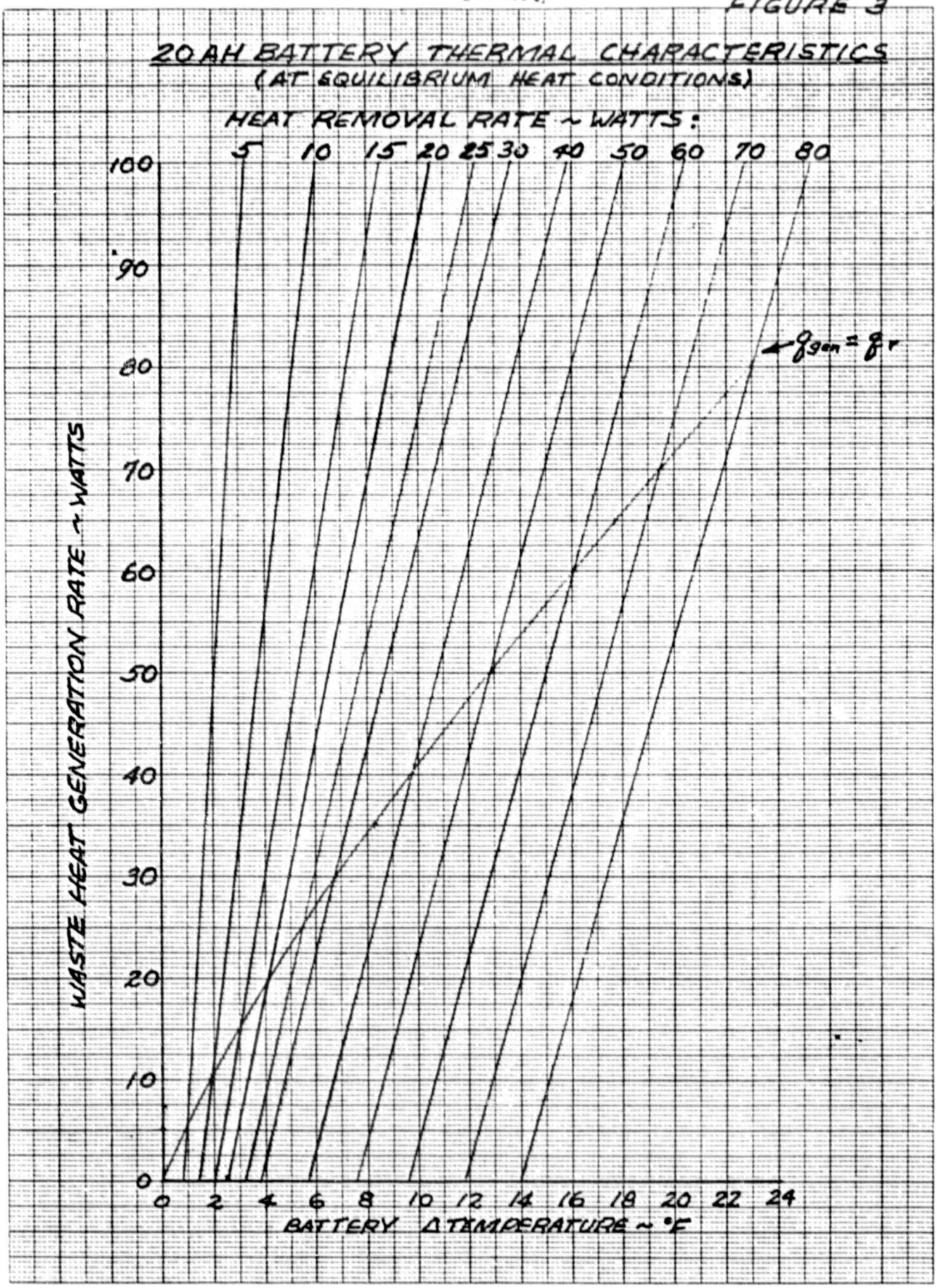

FIGURE 4

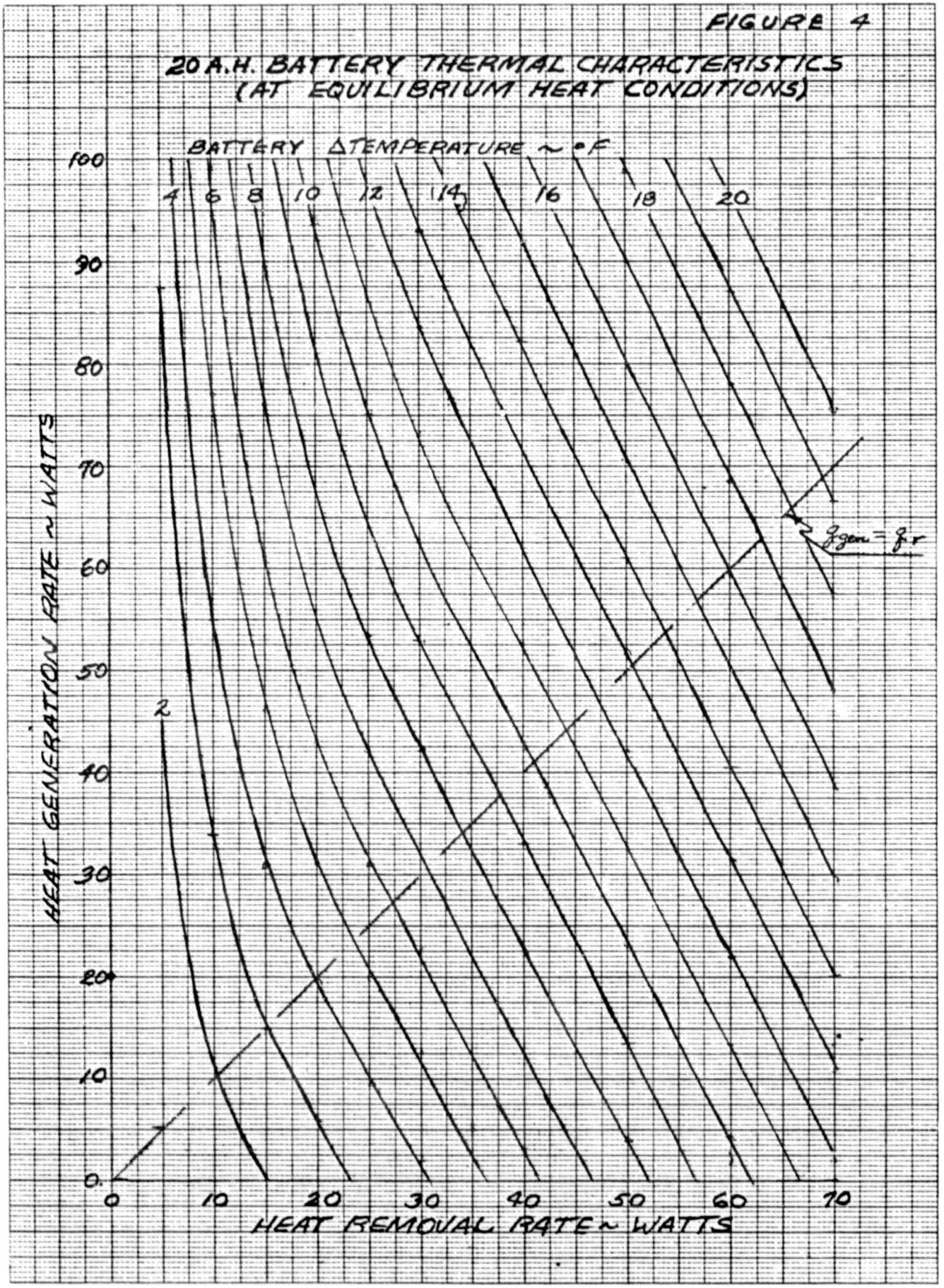

10/21/81

FIGURE 5

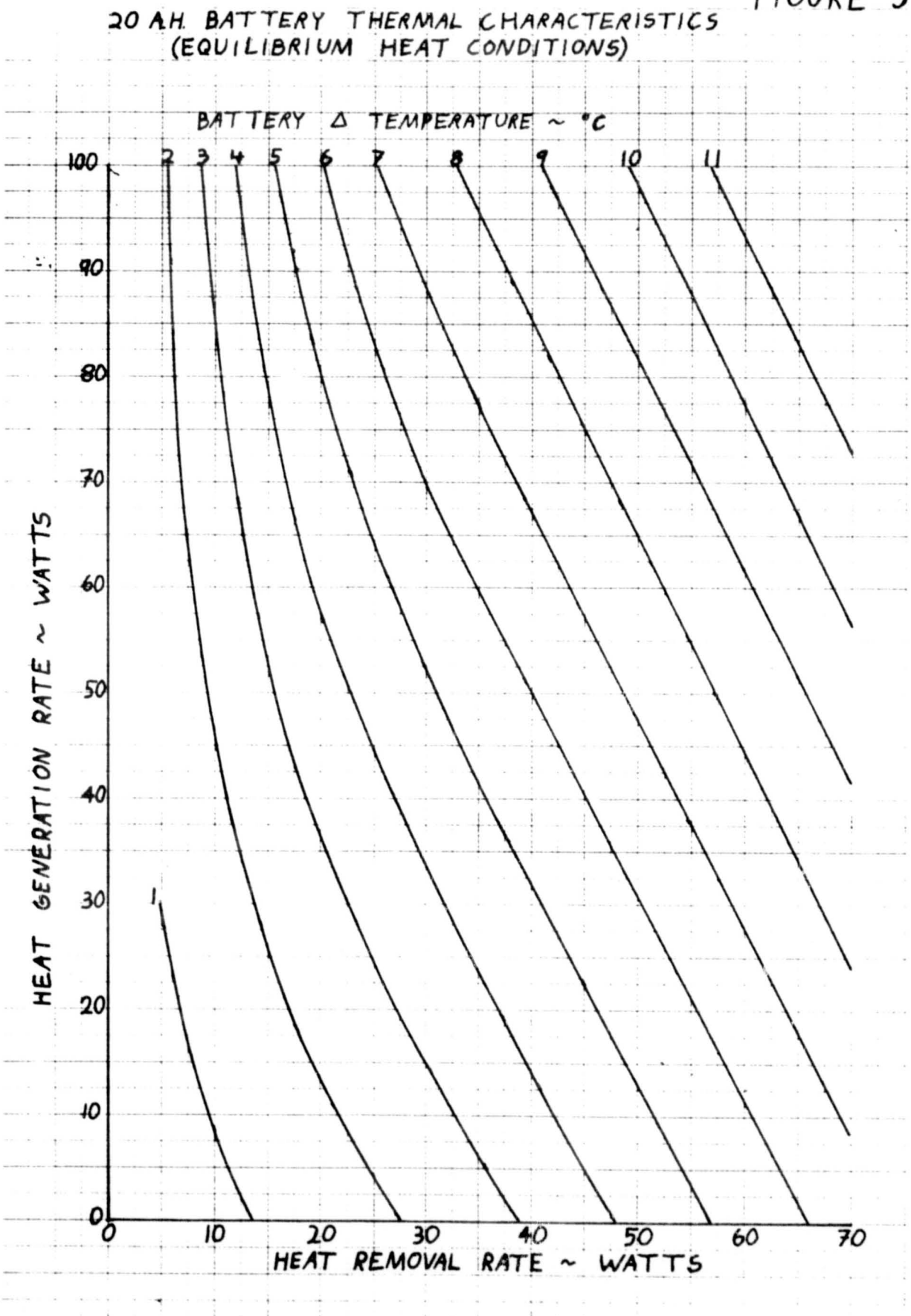

FIGURE 6

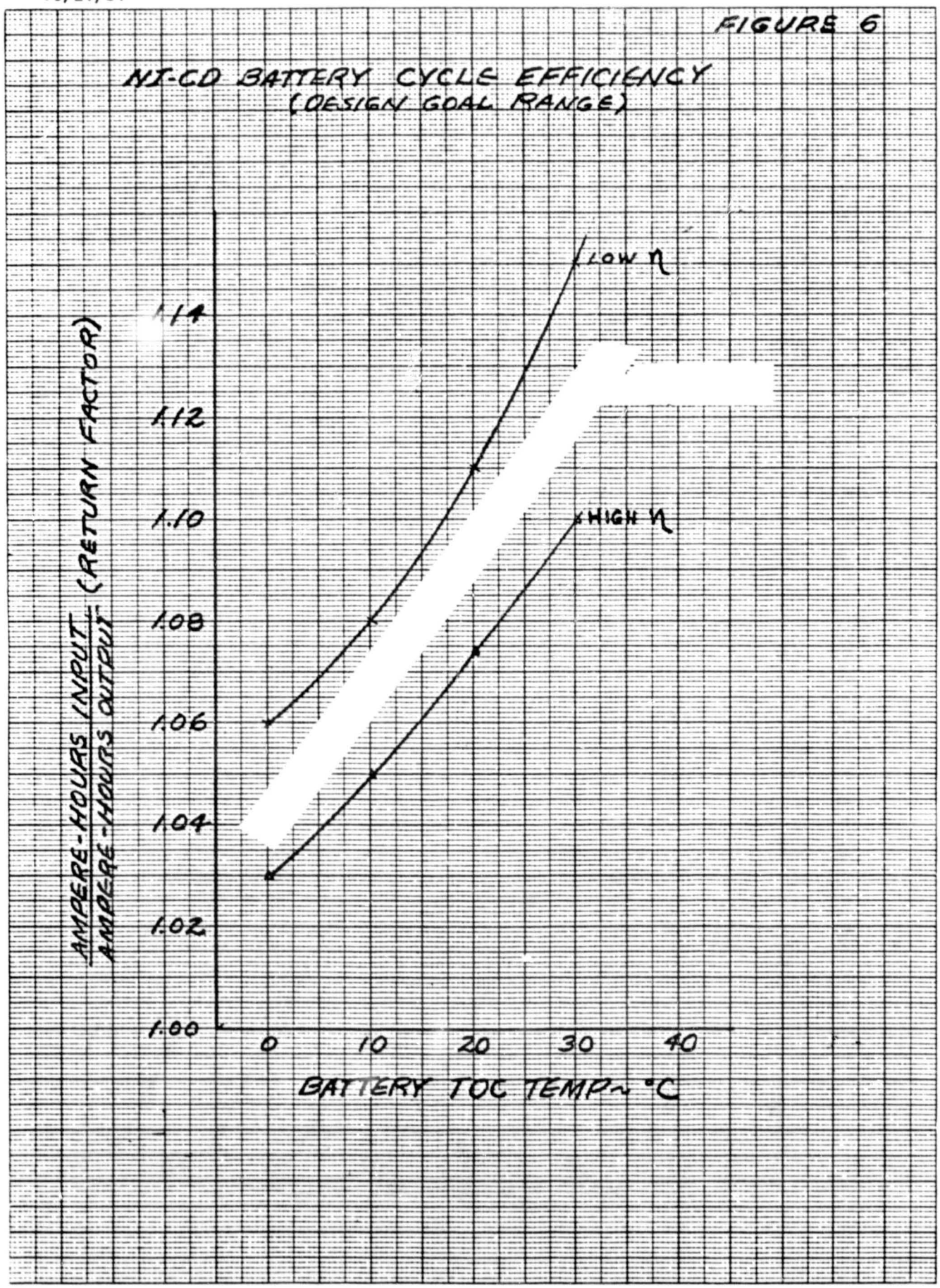

FIGURE 6A

10/21/81

AVERAGE CHARGE TO DISCHARGE VOLTAGE RATIOS

NOTES

- BASED ON ACCEPT. TEST DATA FROM SMM FLIGHT BATTERIES.
- C/2 AMP CHARGE RATE TO VOLT LIMIT, THEN VOLT LIMIT TO END OF CYCLE.
- 25% DEPTH OF DISCHARGE CYCLES.
- 90 MIN CYCLES, 30 MIN. DISCHARGE. VOLTAGE LIMIT S711-16 CURVE 6.

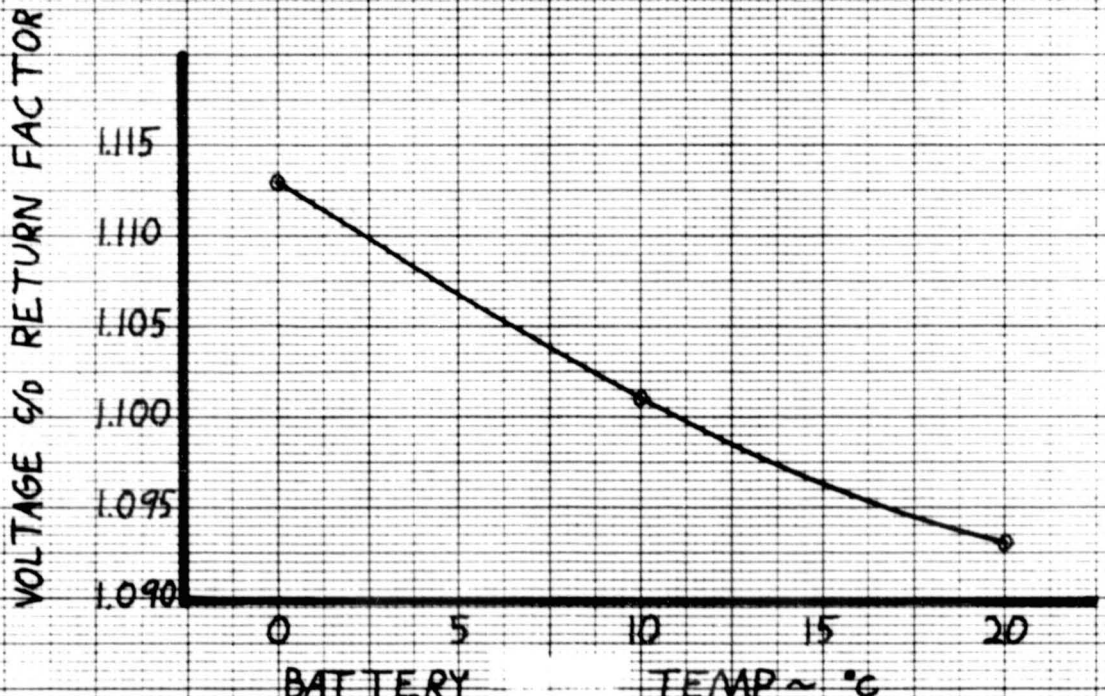

10/21/81

FIGURE 6B

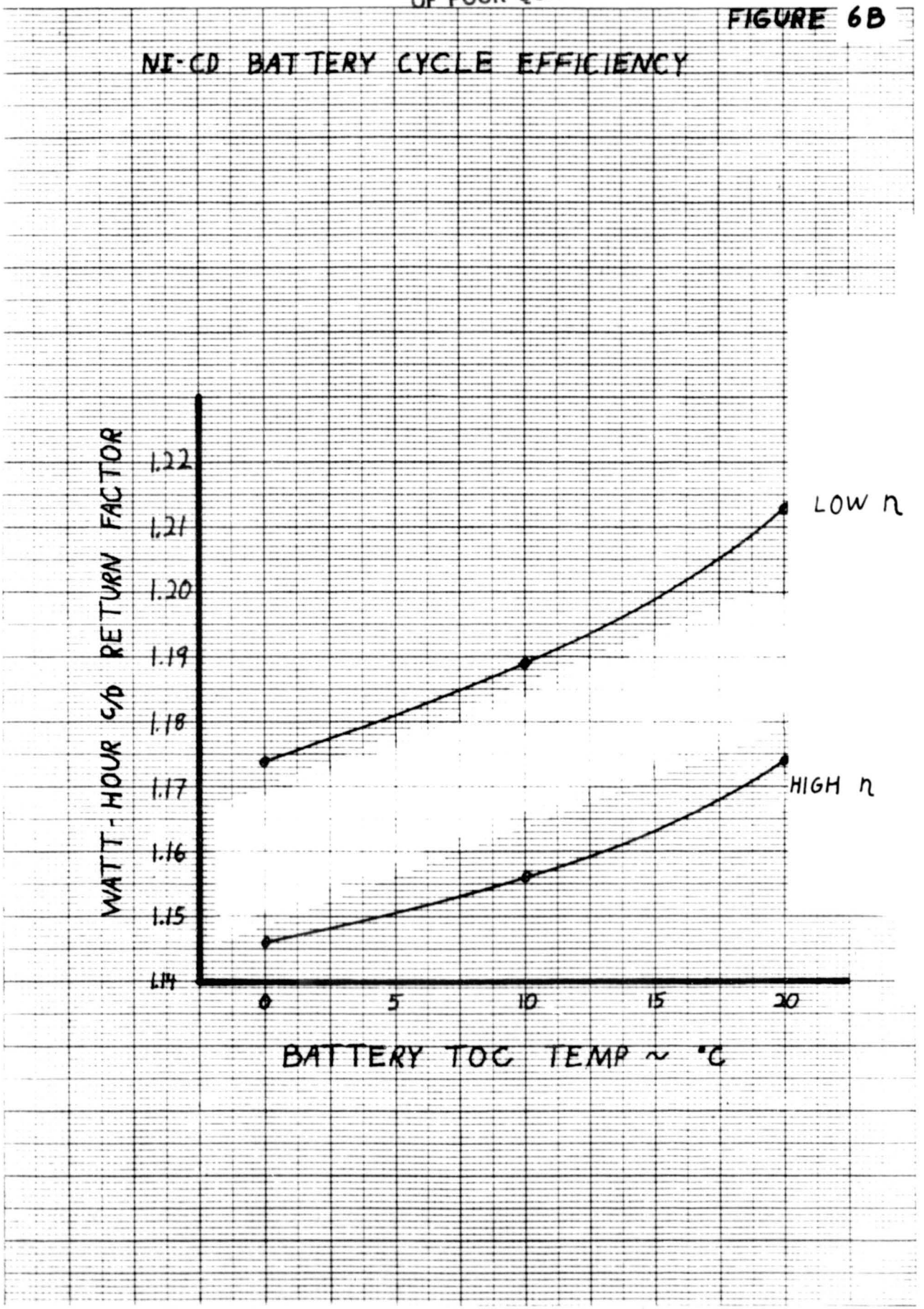

FIGURE 7

20 A.H. BATTERY THERMAL CHARACTERISTICS
(EQUILIBRIUM HEAT CONDITIONS)
WITH OPERATING LIMITS FOR LOW EARTH ORBIT

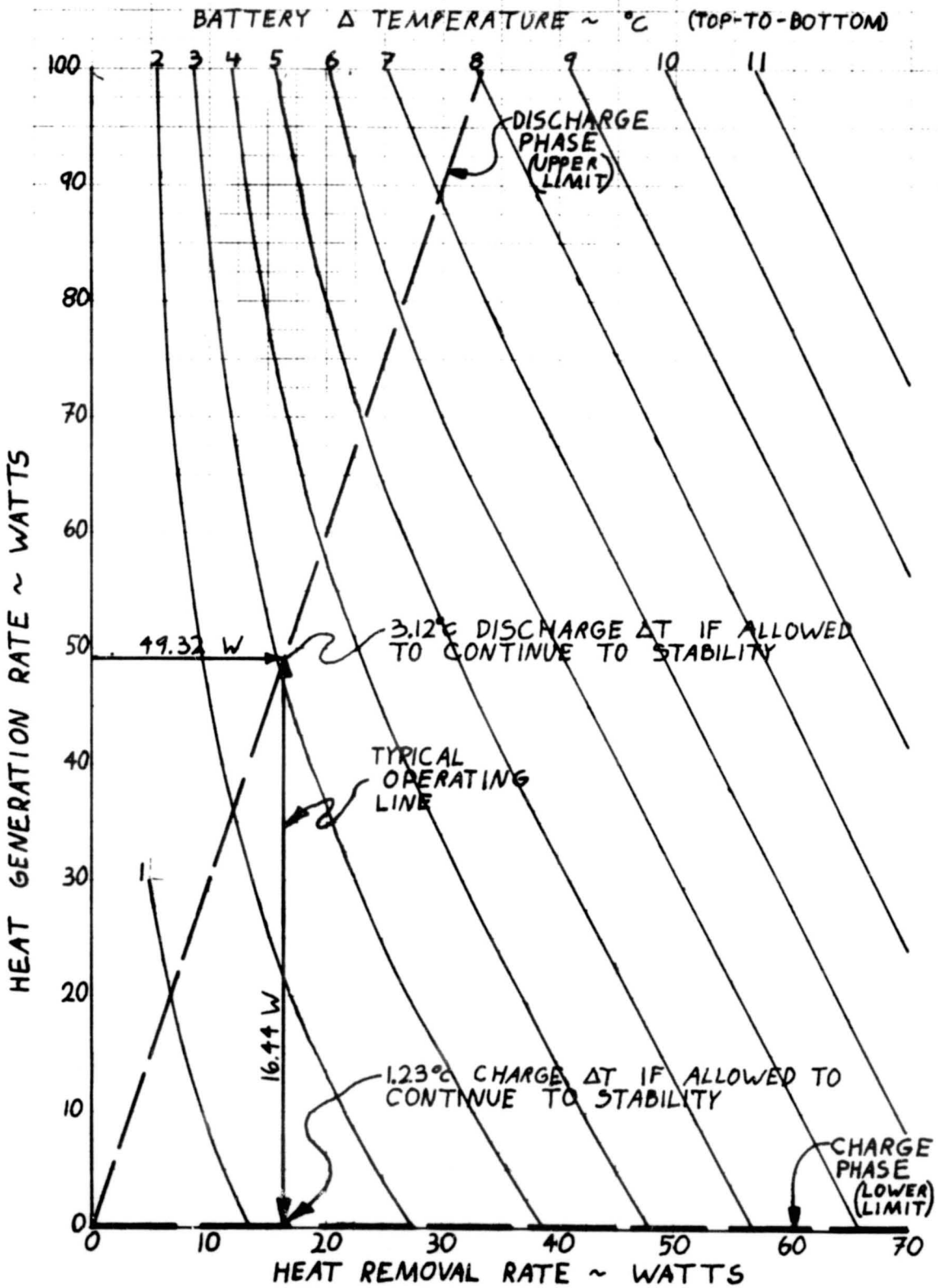

FIGURE 8

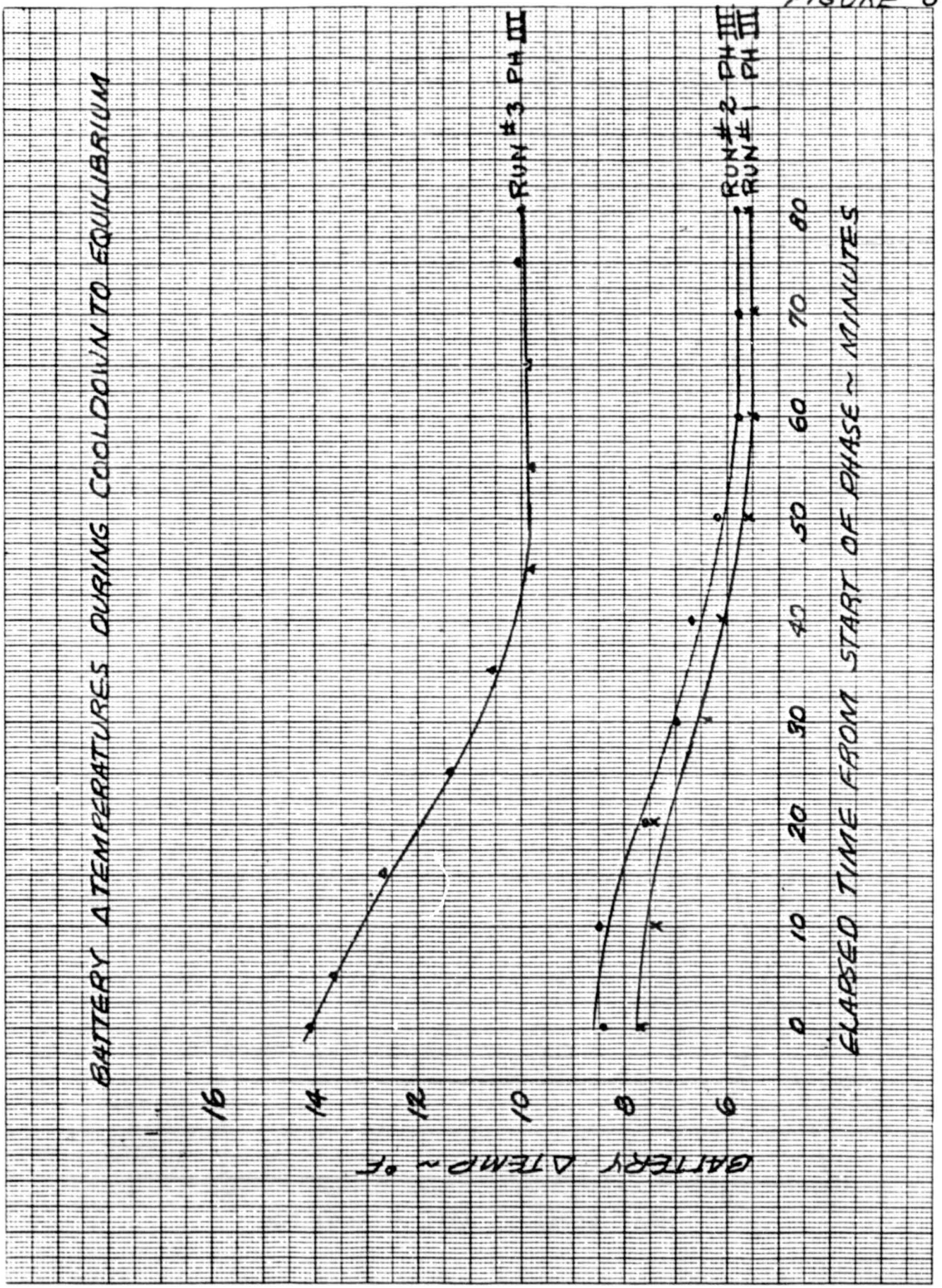

FIGURE 9

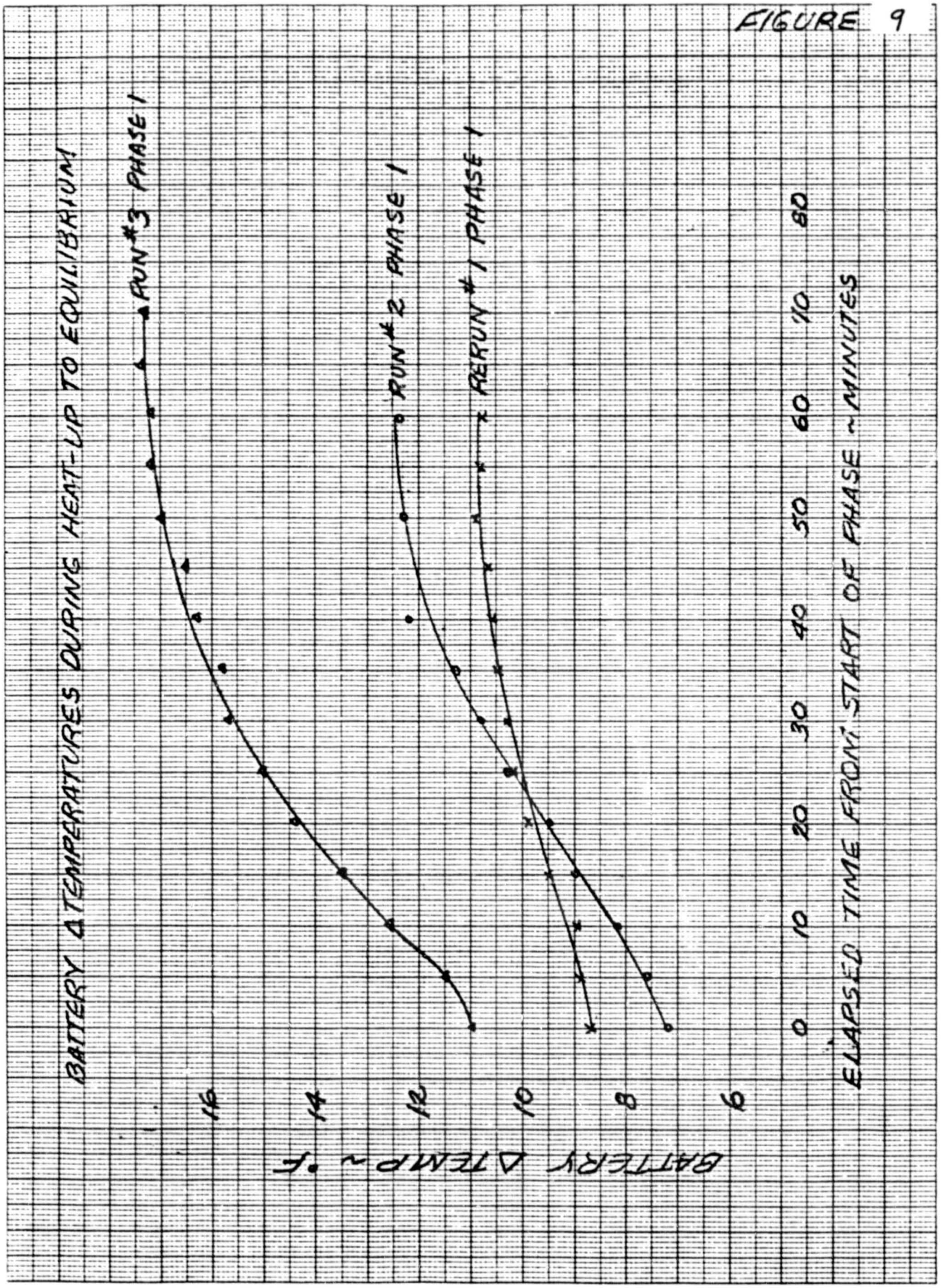

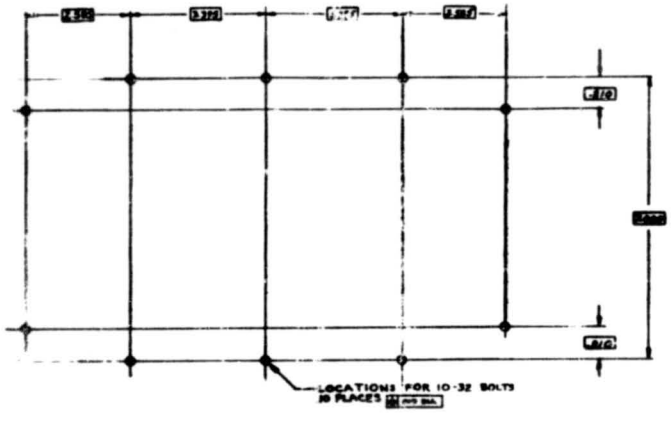

BATTERY MOUNTING DIMENSIONS

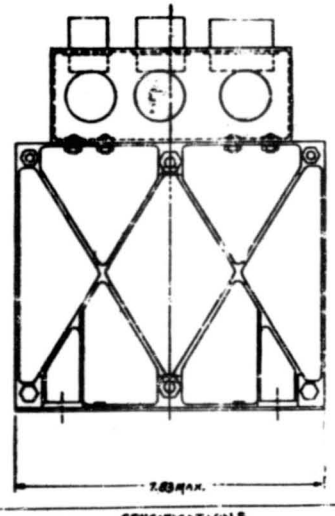

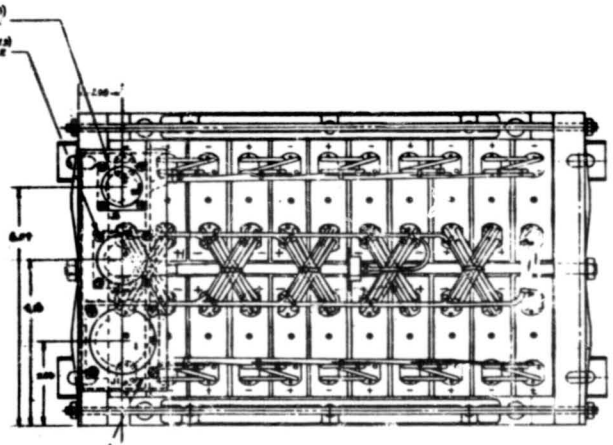

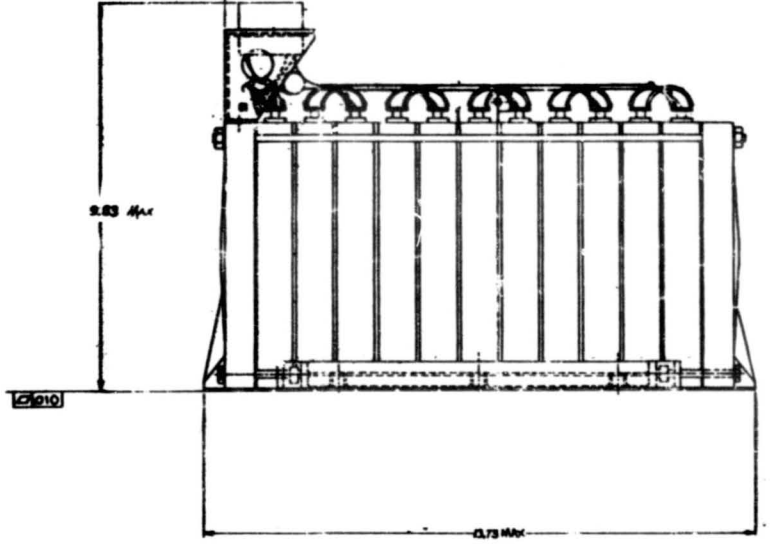

SPECIFICATIONS

NOMINAL CAPACITY	20AH @ 2 HOUR RATE	TEMPERATURE SENSING	(1) PRECISION PLATINUM THERMISTOR OR THERMOCOUPLE (2) THERMO-OPTIC SWITCH
NUMBER OF CELLS	22		
OUTLINE DIMENSIONS	26.7 cm (10.5 in) X 18.8 cm (7.4 in) X 28.9 cm (11.4 in)	STATE-OF-CHARGE SENSING	(1) SIGNAL ELECTRONIC CELL/BATTERY
NOMINAL WEIGHT	25.8 kg (57.0 lb)	THERMAL CONTROL	PASSIVE
MANUFACTURER	MCDONNELL DOUGLAS ASTRONAUTICS CO EAST	OPERATING TEMPERATURE	0° C TO 30° C NOMINAL
PEAK DISCHARGE RATE	60A FOR 2 min.	NOMINAL DISCHARGE VOLTAGE	26.4 V
RECOMMENDED DISCHARGE RATE	20A	NOMINAL CHARGE VOLTAGE	29.80V @ C/10 RATE
		TERMINALS	ISOLATED FROM CASE

NASA STANDARD 20 AH NI-CD SPACECRAFT BATTERY ENVELOPE DRAWING		
SIZE E	CODE IDENT NO.	77J237003